# Athens Journal of Sciences

*Quarterly Academic Periodical, Volume 11, Issue 1, March 2024*
*URL: https://www.athensjournals.gr/ajs*
*Email: journals@atiner.gr*
*e-ISSN: 2241-8466 DOI: 10.30958/ajs*


## Front Pages


*MANFRED RÖSSLE & STEFAN POHL*

**Quality Testing in Aluminum Die-Casting – A Novel Approach using Acoustic Data in Neural Networks**

*CHRISTOPH SCHATTSCHNEIDER, SINA PIONTEK, HANNES JACOBS, ANDREA BÖHME, CONCETTA SIRENA & ANDREAS FOITZIK*

**Proof of Principle of Wastewater Treatment using Plasma Discharge to Reduce the Amount of Methylparaben**

*NATALLIA YANKEVICH*

**Algorithm for Control of Traffic Flow in an Intelligent Transport System**

*KUMUDIKA K.E. PERERA*

**An Analysis of Stream Flow and Flood Frequency: A Case Study from Downstream of Kelani River Basin, Sri Lanka**

# Athens Journal of Sciences

*Published by the Athens Institute for Education and Research (ATINER)*



**********

*ATINER is an Athens-based World Association of Academics and Researchers based in Athens. ATINER is an independent and non-profit Association with a Mission to become a forum where Academics and Researchers from all over the world can meet in Athens, exchange ideas on their research and discuss future developments in their disciplines, as well as engage with professionals from other fields. Athens was chosen because of its long history of academic gatherings, which go back thousands of years to Plato's Academy and Aristotle's Lyceum. Both these historic places are within walking distance from ATINER's downtown offices. Since antiquity, Athens was an open city. In the words of Pericles, Athens"…is open to the world, we never expel a foreigner from learning or seeing". ("Pericles' Funeral Oration", in Thucydides, The History of the Peloponnesian War). It is ATINER's mission to revive the glory of Ancient Athens by inviting the World Academic Community to the city, to learn from each other in an environment of freedom and respect for other people's opinions and beliefs. After all, the free expression of one's opinion formed the basis for the development of democracy, and Athens was its cradle. As it turned out, the Golden Age of Athens was in fact, the Golden Age of the Western Civilization. Education and (Re)searching for the 'truth' are the pillars of any free (democratic) society. This is the reason why Education and Research are the two core words in ATINER's name.*

**********

The ***Athens Journal of Sciences (AJS)*** is an Open Access quarterly double-blind peer reviewed journal and considers papers from all areas of Natural & Formal Sciences, including papers on agriculture, computer science, environmental science, materials science, transportation science, chemistry, physics, mathematics and statistics, biology, geography, and earth science (geology, oceanography, astronomy, meteorology). Many of the papers published in this journal have been presented at the various conferences sponsored by the Natural & Formal Sciences Division of the Athens Institute for Education and Research (ATINER). All papers are subject to ATINER's Publication Ethical Policy and Statement.

The Athens Journal of Sciences
ISSN NUMBER: 2241-8466- DOI: 10.30958/ajs
Volume 11, Issue 1, March 2024
Download the entire issue (PDF)

**Front Pages** i-viii

**Quality Testing in Aluminum Die-Casting – A Novel Approach using Acoustic Data in Neural Networks** 9
*Manfred Rössle & Stefan Pohl*

**Proof of Principle of Wastewater Treatment using Plasma Discharge to Reduce the Amount of Methylparaben** 29
*Christoph Schattschneider, Sina Piontek, Hannes Jacobs, Andrea Böhme, Concetta Sirena & Andreas Foitzik*

**Algorithm for Control of Traffic Flow in an Intelligent Transport System** 39
*Natallia Yankevich*

**An Analysis of Stream Flow and Flood Frequency: A Case Study from Downstream of Kelani River Basin, Sri Lanka** 55
*Kumudika K.E. Perera*

# Athens Journal of Sciences
# Editorial and Reviewers' Board

# President's Message

All ATINER's publications including its e-journals are open access without any costs (submission, processing, publishing, open access paid by authors, open access paid by readers etc.) and is independent of presentations at any of the many small events (conferences, symposiums, forums, colloquiums, courses, roundtable discussions) organized by ATINER throughout the year and entail significant costs of participating. The intellectual property rights of the submitting papers remain with the author. Before you submit, please make sure your paper meets the basic academic standards, which includes proper English. Some articles will be selected from the numerous papers that have been presented at the various annual international academic conferences organized by the different divisions and units of the Athens Institute for Education and Research. The plethora of papers presented every year will enable the editorial board of each journal to select the best, and in so doing produce a top-quality academic journal. In addition to papers presented, ATINER will encourage the independent submission of papers to be evaluated for publication.

The current issue is the first of the eleventh volume of the *Athens Journal of Sciences (AJS),* published by Natural & Formal Sciences Division of ATINER.

Gregory T. Papanikos, President, ATINER.

**12th Annual International Conference on Chemistry**
**22-25 July 2024, Athens, Greece**

The Natural Sciences Unit of ATINER, will hold its **12th Annual International Conference on Chemistry, 22-25 July 2024, Athens, Greece** sponsored by the Athens Journal of Sciences. The aim of the conference is to bring together academics and researchers of all areas of chemistry and other related disciplines. You may participate as stream organizer, presenter of one paper, chair a session or observer. Please submit a proposal using the form available (https://www.atiner.gr/2023/FORM-CHE.doc).

**Academic Members Responsible for the Conference**

- **Dr. Haiduke Sarafian**, Head, Natural Sciences Unit, ATINER & Professor of Physics and Endowed Chair of John T. and Paige S. Smith Professor of Science, Pennsylvania State University, USA.

**Important Dates**

- Abstract Submission: **2 April 2024**
- Acceptance of Abstract: 4 Weeks after Submission
- Submission of Paper: **24 June 2024**

**Social and Educational Program**

The Social Program Emphasizes the Educational Aspect of the Academic Meetings of Atiner.

- Greek Night Entertainment (This is the official dinner of the conference)
- Athens Sightseeing: Old and New-An Educational Urban Walk
- Social Dinner
- Mycenae Visit
- Exploration of the Aegean Islands
- Delphi Visit
- Ancient Corinth and Cape Sounion

**Conference Fees**

Conference fees vary from 400€ to 2000€
Details can be found at: https://www.atiner.gr/fees

**12th Annual International Conference on Physics**
**22-25 July 2024, Athens, Greece**

The Natural Sciences Unit of ATINER, will hold its **12th Annual International Conference on Physics, 22-25 July 2024, Athens, Greece** sponsored by the Athens Journal of Sciences. The aim of the conference is to bring together academics and researchers of all areas of physics and other related disciplines. Please submit a proposal using the form available (https://www.atiner.gr/2023/FORM-PHY.doc).

**Important Dates**

- Abstract Submission: **2 April 2024**
- Acceptance of Abstract: 4 Weeks after Submission
- Submission of Paper: **24 June 2024**

**Academic Member Responsible for the Conference**

- **Dr. Haiduke Sarafian**, Head, Natural Sciences Unit, ATINER & Professor of Physics and Endowed Chair of John T. and Paige S. Smith Professor of Science, Pennsylvania State University, USA.

**Social and Educational Program**

The Social Program Emphasizes the Educational Aspect of the Academic Meetings of Atiner.

- Greek Night Entertainment (This is the official dinner of the conference)
- Athens Sightseeing: Old and New-An Educational Urban Walk
- Social Dinner
- Mycenae Visit
- Exploration of the Aegean Islands
- Delphi Visit
- Ancient Corinth and Cape Sounion

More information can be found here: https://www.atiner.gr/social-program

**Conference Fees**

Conference fees vary from 400€ to 2000€
Details can be found at: https://www.atiner.gr/fees

*Athens Journal of Sciences- Volume 11, Issue 1, March 2024 – Pages 9-29*

# Quality Testing in Aluminum Die-Casting – A Novel Approach using Acoustic Data in Neural Networks

*By Manfred Rössle[*] & Stefan Pohl[±]*

*In quality control of aluminum die casting various processes are used. For example, the density of the parts can be measured, X-ray images or images from the computed tomography are analyzed. All common processes lead to practically usable results. However, the problem arises that none of the processes is suitable for inline quality control due to their time duration and to their costs of hardware. Therefore, a concept for a fast and low-cost quality control process using sound samples is presented here. Sound samples of 240 aluminum castings are recorded and checked for their quality using X-ray images. All parts are divided into the categories "good" without defects, "medium" with air inclusions ("blowholes") and "poor" with cold flow marks. For the processing of the generated sound samples, a Convolutional Neuronal Network was developed. The training of the neural network was performed with both complete and segmented sound samples ("windowing"). The generated models have been evaluated with a test data set consisting of 120 sound samples. The results are very promising. Both models show an accuracy of 95% and 87% percent, respectively. The results show that a new process of acoustic quality control can be realized using a neural network. The model classifies most of the aluminum castings into the correct categories.*

**Keywords:** *acoustic quality control, aluminum die casting, convolutional neural networks, sound data*

## Introduction

A fast and cost-efficient quality control plays a central role in manufacturing companies. Modern methods open completely new possibilities for designing such processes. Recording a wide variety of data and processing it with innovative technologies helps to gain new insights. These include technologies such as neural networks, which belong to the wide field of artificial intelligence.

Frequently used methods of quality assurance for aluminum castings are computed tomography and X-ray of the parts. This involves taking images of the parts to be inspected to detect any defects, such as air pockets ("blowholes") or cracks. Taking a computed tomography scan is lengthy compared to process times. With an average process time of about 30 seconds per piece, a recording time of 20-30 minutes (!) per piece is clearly too long so that an inline process control is not feasible in a meaningful way.

To create a new inline-capable process of quality assurance, it will be examined whether the use of sound data processing with neural networks is a viable way.

[*]Professor, Department of Business Information Systems, Aalen University of Applied Sciences, Germany.
[±]Carl-Zeiss AG, Germany.

Based on the idea that bodies with different densities produce different sounds and frequencies, it is assumed that manufacturing defects, such as air pockets or cracks, change the density of the parts and this can be identified by the neural network. The resulting process could be integrated into an existing manufacturing process at low cost.

## Related Work

In recent years, there has been great progress in the field of artificial intelligence. One of these fields is audio data processing in neural networks. Examples are speech, music and pattern recognition in audio files, as well as audio classification. Many application examples can already be found in practice today. For the processing of sound data there are a variety of possibilities, which differ depending on the problem. For audio classification, image representation and processing of audio data, among others, have shown promise (Boddapati et al. 2017, Khamparia et al. 2019, Piczak 2015, Salamon and Bello 2017). Other approaches investigate the processing of raw audio data, without the prior extraction of imaging or manually created features (Abdoli et al. 2019, Yuji Tokozume 2017). The raw audio data is directly provided as input to the neural network. Thus, the processing is not exclusively limited to audio signals, but also applicable to other digital signals like vibration.

When processing the imaged audio signals, the spectrogram, Mel spectrogram or Mel Frequency Cepstral Coefficient (MFCC) are often used. The resulting image representations can be further processed like conventional images in neural networks. Good results in image recognition have been obtained mainly with Convolutional Neural Networks (CNNs) (Krizhevsky et al. 2017). However, CNNs are also used in the processing of raw audio signals.

In most measurement methods, the audio data is processed as a complete block. Another possibility is to divide the audio file into several segments and make them available to the neural network. In this case, the individual segments are classified and later merged for the overall result (Hassan et al. 2019).

Specific approaches for quality assurance of aluminum die-castings using audio data in neural networks cannot be found in the literature. However, other interesting methods for quality control using neural networks are available. Examples are automated quality control of aluminum castings (Mery 2020), (Nguyen et al. 2020) or automated localization of casting defects (Nie et al. 2017) based on X-ray images and their processing in CNNs.

There are concrete approaches for acoustic quality and condition control. For example, the quality of welds (Lv et al. 2017), ceramic tiles (Cunha et al. 2018), the condition of gearboxes (Jing et al. 2017), machines (Kothuru et al. 2019), wind turbines (Kong et al. 2020) or hydropower plants (Voith 2020) can be tested acoustically. A very exotic approach is acoustic quality testing of dried strawberries, to distinguish ripe from overripe fruit (Przybył et al. 2020).

## Design and Execution of the Research Process

This chapter describes the design and execution of the research process. After a description of the used aluminum parts and the process of obtaining the sound samples, a derivation of the architecture of the neural network and a description the execution of the experiments follows.

*Design of Experiments*

Description of the Aluminum Parts

The aluminum castings are provided by the foundry of Aalen University. They are manufactured using the aluminum die-casting process. A total of 240 parts are available for creating sound samples. Each part measures 19.8 x 14.8 x 0.4 cm. The parts are each casted with a defined set of parameters. These parameters are chosen very "extreme", so that the desired properties of the categories described below are achieved in every case.

All castings are checked for quality by means of X-ray images and labeled accordingly by die-casting experts. This labeling allows each part to be assigned without doubt to one of the three categories. The number of parts is the same for each category. There are 80 parts assigned to each category.

- Category "good"

The parts in the "good" category have optimum die-casting parameters. No defects in the form of white spots are visible on the respective X-ray image.

- Category "medium"

Parts in the "medium" category have a changeover point that is too early. This leads to blow holes in the material. Defects in this category cannot be detected visually in the X-ray image or are very difficult to detect. They manifest themselves in barely visible white spots.

- Category "poor"

Parts in the "poor" category have too low gating speed. Typical defects are cold flow marks, which can be perceived as bright spots in the X-ray image. Unlike aluminum parts in the "good" and "medium" categories, these parts can be visually distinguished from the others because they have an uneven surface.

Recording of Sound Samples

The sound samples were recorded in the soundproof room of the Faculty of Optometry and Hearing Acoustics at Aalen University. This offers optimal conditions for the recordings without interfering noise. The recording equipment was also provided by Aalen University and consisted of a professional recording device (Zoom Handy Recorder H4n) and an ECM8000 measurement microphone from Behringer. The recordings were made in WAV format with 96 kHz and a depth of 24 bits.

**Figure 1. Design of Experiment**

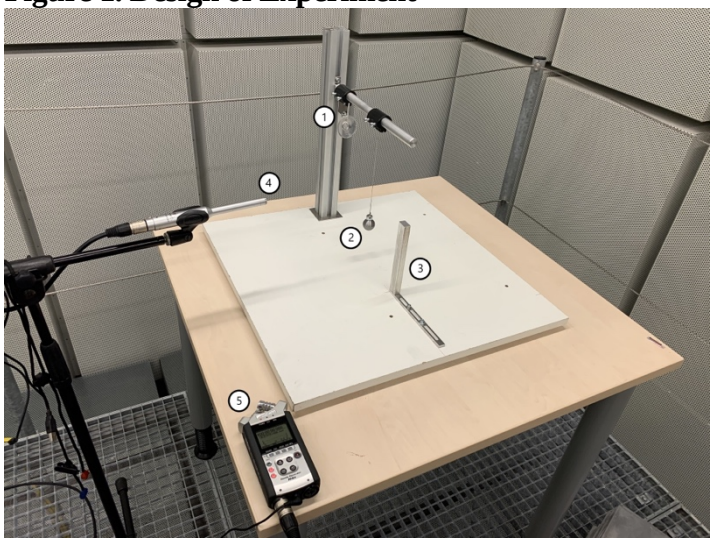


Figure 1 shows the setup with the holding device and the equipment used. The following elements can be seen in the image:

1. Suction cup for fixing the aluminum castings
2. Pendulum with aluminum ball
3. Wedge for constant force application of the pendulum
4. Microphone
5. Recording device

The holding fixture was specially designed and manufactured to record the sound samples. This guarantees a consistent environment for holding each aluminum casting.

The suction cup (1) ensures that the damping of the vibrations on the aluminum casting after the pendulum (2) has bounced is as low as possible. This allows the sound to propagate in the best possible way. The pendulum ball is an aluminum ball, held by a cord on a crossbar to the aluminum casting. A wedge (3) ensures that the acting force of the pendulum on the aluminum casting remains as constant as possible. The resulting sound, which is transmitted through the air, is then recorded in mono via a microphone (4) and stored as a WAV file on the recording device (5).

Recording continues for a few seconds to capture any after-oscillations. The resulting "silence" at the beginning and end of each recording, must be removed during data pre-processing. Since the recording device must be operated manually, the actual length of each sound sample varies approximately between five and seven seconds.

Due to the small number of pieces and the resulting relatively small data set, two sound samples are taken from each aluminum casting. No changes are made to the recording parameters. The resulting data set contains a total of 480 sound samples in the form of digital audio files. However, these cannot be used immediately for the analysis, as they have to be processed beforehand.

Determination of a Suitable Architecture of the Neural Network

There are many different types of neural networks to choose from. Not every type is equally well suited for the problem under investigation. Suitable types can be identified by analyzing previous investigations. The most common types of neural networks for audio data processing are (Purwins et al. 2019, p. 10):

- Convolutional Neural Networks
- Recurrent Neural Networks
- Convolutional Recurrent Neural Networks

As the literature review shows, there are no significant differences between the types in terms of their results in audio data classification. However, there are differences in performance of data processing and model evaluation. For example, Convolutional Neural Networks have an advantage in this area (Purwins et al. 2019, p. 10).

After the selection of the type has been made, the identification of the architecture of the network can be carried out. Unlike the previously mentioned points, the structure of the network architecture is subject to the circumstances of the investigation. Depending on the data set, the structure of the network may vary. Using the same data set different architectures can lead to different results.

It makes sense to follow proven architectures and adapt them to the needs of the project. The choice of architecture depends, among other things, on the type of data and the size of the data set. Since the data to be processed changes with the selection of the audio feature, the appropriate choice of it should also be considered.

Again, previous research in audio classification provides clues for an architecture. Costa et al. (2017, p. 34) as well as Huzaifah (2017, p. 3), show an approach with convolutional layers followed by a max-pooling layer. With each Convolutional Layer, the number of filters increases. Several Fully Connected Layers are used for classification. Figure 2 Approach A shows the described structure.

Another interesting approach, illustrated in Figure 2 Approach B, is shown by Lai et al. (2018, p. 359) with two consecutive convolutional layers, each followed by a max-pooling layer. Again, the number of filters increases with each Convolutional Layer. The end is again formed by several Fully Connected Layers. This approach is inspired by the well-known architecture VGG Net (Simonyan and Zisserman 2014, p. 3). Both approaches follow the structure presented by Salamon and Bello (2017, p. 280) and Piczak (2015, p. 3).

**Figure 2. Architectures of CNNs**

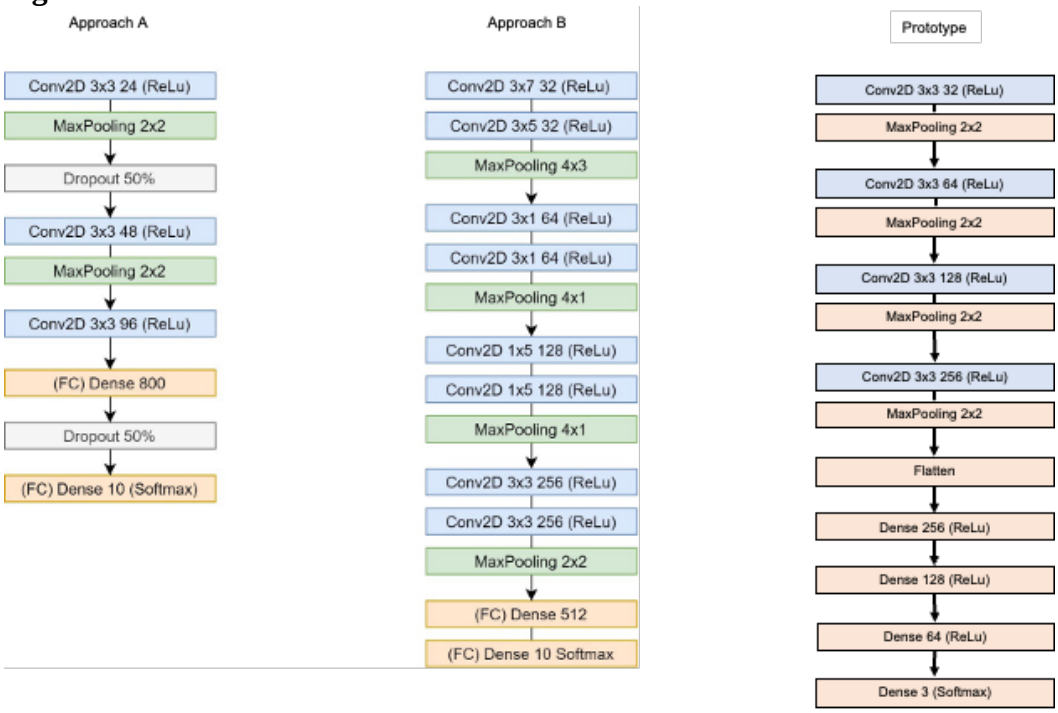


*Source:* Approach A: Huzaifah (2017, p. 3), Approach B: Lai et al. (2018, p. 359). Prototype: Authors.

Based on the findings reported above, a prototype of a CNN was developed as shown in Figure 2 (Prototype). The different areas are divided into several blocks for more clarity.

The first layer of the neural network is the input layer. It receives as input the image representation of the sound samples in the form of the calculated Mel-Frequency Cepstral Coefficients. This is followed by several identical blocks each consisting of a Convolutional Layer and a MaxPooling Layer. A total of four of these blocks are built into the neural network. Each convolutional layer of these blocks uses a different number of filters. This doubles with each subsequent layer. The first block starts with 32 filters and the last block ends with 256 filters. Their task is to recognize features and patterns from the input data.

Once the four blocks have been run through, an attempt is made to perform a classification based on the information learned from the input data. To do this, the data must first be unrolled ("flattened") and transformed from multidimensional to one-dimensional data structures. The connection of all neurons of the input and output layers takes place in the so-called "Dense Layer". A total of four of these are used in the neural network. Unlike in the blocks before, the number of units decreases with each layer. The first Dense Layer has 256 units, the last three. As can be seen, the last Dense Layer has as many units as there are possible classes.

Selection of suitable audio features

Certain specific audio features have also shown promise in the past. The most common audio features are raw audio data, spectrograms, Mel-Frequency Cepstral Coefficients, and Log-Mel Spectrograms, whereby Mel-Frequency Cepstral

Coefficients and Log-Mel Spectrograms are the most commonly used features in audio data processing (Purwins et al. 2019, p. 10). They produce, in contrast to the raw audio data, a more compact representation of the information. This leads to better performance in training and processing the data by the neural network. However, these features need to be computed by defined functions, which may lead to a loss of information (Purwins et al. 2019, p. 10).

Based on the explained points, the choice of the network type falls on the Convolutional Neural Network and the choice of the audio feature on the Mel-Frequency Cepstral Coefficients. The combination of CNN and MFCC has proven to be a promising basis in the past, provided very good results.

*Execution of the Research Process*

Preprocessing of Audio Data

The generated sound samples must be preprocessed before being given as input to the neural network. The sound samples used for training the neural network as well as for evaluation and testing must always have the same length. If all audio files are considered, the file with the shortest recording duration is 5.8 seconds and the file with the longest recording duration is 9.6 seconds.

To ensure that all sound samples have the same recording duration, they are cut both at the beginning and at the end. A self-developed function is used to cut the audio files. It removes areas that are below a specified threshold. This threshold applies only to values located at the beginning and end of the file, but not to values located between relevant information of the audio file.

Since the function distinguishes relevant from irrelevant information based on the amplitude values, an additional parameter must be passed for a constant length of each file. This parameter defines a fixed length for each audio file, even if the amplitude value was already undercut before this value.

Specifically this means that if, for example, an audio file falls below the amplitude value after three seconds, but the parameter sets a length of five seconds, the audio file will not be truncated until that later point. This guarantees a constant length of five seconds of each audio file.

Maintaining a constant length is essential for training the neural network. For an error-free training process, each file must have the same input format. All audio files that are passed to the generated model for prediction must correspond to this input format.

The sound samples are recorded with a sampling rate of 96 kHz. The transformation into the time-frequency spectrum reveals in which frequency range the relevant information is located. In our case, most of the information is found in the range between 0 Hz and 8,000 Hz.

The sampling rate is reduced from 96 kHz to 16 kHz. This results in a reduction of the amount of data, which leads to a faster processing of the sound samples. The sampling rate reduction is done with the help of a so-called resampling function. This takes over the reduction of the sampling rate after the cutting process and saves the files as new audio files.

Since the files before and after the sampling rate reduction differ widely in their properties, they are compared in Table 1. Besides the changed parameters, such as sampling rate and fixed length, especially the size of the individual audio data has decreased considerably.

**Table 1. Properties of Raw and Preprocessed Samples**

| | **Before Reduction** | **After Reduction** |
|---|---|---|
| Sampling rate | 96 kHz | 16 kHz |
| Length | between 5.8 and 9.6 seconds | 5 seconds |
| Size | between 3.2 and 5.3 Megabyte | 0.313 Megabyte |

Training of the Neural Network

The neural network is trained using two different methods. At first, the neural network processes the audio files from the training data set without modification and in full length. In the second method, random regions (segments) of equal length are taken from the sound samples and passed to the neural network for training. The relatively small data set can be artificially enriched using this method.

- Complete sound samples

With this method, the sound samples are used as a complete block. For this purpose, the MFCC coefficient of the entire sound sample is calculated. The 360 samples thus obtained are passed to the neural network for training.

- Segmented sound samples

To artificially increase the size of the data set for training, random segments of equal size are taken from each sound sample. Both the placement of the section within the sound sample and the choice of the sound sample itself, happens randomly. A two-second segment is then taken from each sound sample. The MFCC coefficient is then determined from this region and passed to the neural network as input.

To obtain the highest possible number of samples of each class, this process is performed 20,000 times. This allows the model to work with 20,000 training data sets.

Training Parameters

Regardless the type of sound sample, the models are trained with 10-fold cross validation. In cross-validation, the entire data set used for training the neural network is divided into k equally sized subsets, where k is the number of subsets (10 in this case). Compared to manually splitting training and validation data, cross-validation is less likely to have an unfavorable distribution of possible classes within the subsets. For the model's overall performance, the average is taken from all obtained metrics (Olson and Delen 2008, p. 141).

The total data set, which consists of 480 sound samples, is manually divided into 75% training and 25% test data. The remaining 360 sound samples in the training data set are subdivided again using 10-fold cross validation. As usual, the subsets are divided into non-overlapping, equal-sized sets of 90% training and 10% validation data each, resulting in 10 training and 10 validation data sets.

The neural network is then trained with the generated segmented data sets. The resulting models can be compared with each other and allow an easier selection of the best model. Table 2 shows the training parameters used for both methods.

**Table 2. Important Parameters of the Models**

| Parameter | Complete sound samples | Segmented sound samples |
|---|---|---|
| Loss function | Categorical Crossentropy | Categorical Crossentropy |
| Optimization function | Adam | Adam |
| Metrics | Accuracy | Accuracy |
| Number of epochs | 30 | 60 |
| Batch size | 32 | 512 |

The loss and optimization functions used are the same for both methods. "Categorical Crossentropy" is selected as loss function and "Adam" (Adaptive Moment Estimation) as optimizer. Also identical is the metric "Accuracy" for both methods. These parameters are chosen based on the research shown in Chapter 2. These have led to be promising results. The specified number of epochs and the batch size have been proven to be optimal by several training runs.

## Results

This section shows the results of the training process and the application of the generated models to the test data set. The first subsection contains a description of how to interpret the results from the training. The necessary steps to generate the predicted values are explained in the second subsection. The results obtained are explained in the third subsection.

### *Evaluation of the Models*

After the successful training of the models, they have to be checked for their performance. The key figures collected during training provide an indication of the expected performance of the model. The two key figures "Accuracy" and "Loss" are decisive for this. They can be used to identify problems such as overfitting or underfitting of the model. Overfitting occurs when the model delivers good results on the training data, but poor results on the test data set. Underfitting occurs when the model delivers poor results on the training data (Wani et al. 2020, pp. 47–48).

For better clarity, these key figures are shown in diagrams. The number of learning cycles is shown on the x-axis and the accuracy and loss values of the training and validation data are shown on the y-axis. In this way, the change in both values over the entire course of the training can be displayed and evaluated.

If the accuracy is considered, both values should ideally rise in a curve and approach the value "1" with increasing number of learning cycles. The curve of the validation data set should run parallel to the curve of the training data set. An emerging gap occurring between training and validation data indicates the overfitting of the model (Moolayil 2019, p. 134).

If, on the other hand, the Loss value is considered, it should decrease with increasing number training cycles. It thus runs in the opposite direction to the accuracy value. The loss values of training and validation data should approach "0" with an increasing number of learning cycles. Here, too, a widening gap between the two curves indicates a problem (Gulli 2017, p. 38).

However, the decisive factor for the performance of the model is the generalization. This tells how good the applicability is to data that the neural network has not yet processed. This is tested with the test data set taken before. As described above, the distribution is 75% training and 25% test data.

Since the membership of each sound sample to a category is known, an accurate evaluation of the results can be performed. Both models, from complete and segmented sound samples, are applied to the test data set and the results are compared.

For this purpose, the probability values of each model are determined for each individual sound sample of the test data set. The exact determination of the values is explained in the following chapter. The higher the determined values match the actual values, the better the performance of the model used.

For a better overview of the results from the test data set, the actual and determined class memberships can be compared in a cross table ("confusion matrix"). For this purpose, the determined classes are listed on the X-axis and the actual classes on the Y-axis in a confusion matrix. Accordingly, an ideal line runs from the top left to the bottom right. Values that are outside this ideal line represent incorrectly classified values. If a model achieves 100% accuracy on the test data set, all values lie on the ideal line.

*Determination of the Probability Values*

The probability values are the results of the model that makes a prediction of class membership. The results are presented in the form of percentages for each possible class. The higher the percentage for a single class, the higher the probability that the sound sample can be assigned to this class. The different classes represent the possible grades (good / medium / poor) of the aluminum castings. To obtain the probability values, the audio data must be processed in advance and the corresponding features extracted. Basically, this is done with the same principle as used for training the model. Depending on whether whole or segmented sound samples are considered, the determination of the probability values looks different.

- Complete sound samples

To determine the probability values of a complete sound sample, the sound sample must be processed as a whole block. For this purpose, the audio file is read in full length and the MFCC coefficient is determined from it. The obtained data is passed to the model for classification. This will lead to the prediction. No further steps need to be performed.

- Segmented sound samples

To classify a segmented sound sample, it is divided into segments. To do this, four segments of equal size, consisting of a two-second window, are taken from the sample.

The distribution of the ranges is not random in this case. Starting with the first range, at the beginning of the sound sample, the remaining ranges follow, each with an offset of one second, until the end of the sound sample. For each of the four areas, the MFCC coefficient is transmitted and the probability values are calculated by the model. The final result of the classification then is the average of all values.

*Results from Training and Test Data*

Below are the results from the training phase and the application to the test data set. The separation is done according to complete and segmented sound samples. Thereby, the sections follow the same scheme. At the beginning, the results of the training phase are presented. From all generated models of the cross validation, the diagrams show the model, with the best performance in each case. For a combined overview, a diagram with the average values of the ten models is shown. Overall training cycles this forms a smoothed representation of the results.

Subsequently, the results of the best model from the application to the test data set are shown. For this purpose, both a confusion matrix and the actually determined probability values for each sound sample are clearly presented in a table.

- Complete sound samples

The course of the accuracy over the 30 training cycles of training and validation data can be seen in Figure 3. Due to the relatively small size of the data set, the course of the validation data is erratic, whereas the curve of the training data runs without major jumps. In the course of the investigation, the maximum number of 30 training cycles, with a given amount of data and structure of the neural network, turns out to be optimal. Further training cycles do not improve the results.

**Figure 3. Model Accuracy and Loss for Complete Sound Samples**

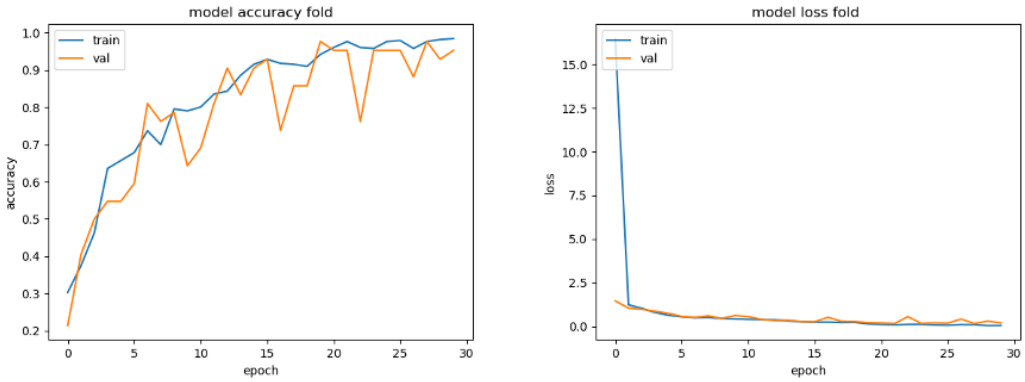

The curves of the loss values in Figure 3 run very flat and parallel to each other without major fluctuations. The fact that the loss value of the validation data does not increase towards the end excludes an overfitting of the model.

For a smoothed course of both curves, the average of all values is shown. This figure contains the values of all ten created models from the cross-validation. Here it can be seen clearly that training and validation accuracy run simultaneously in a curve towards "1". This is also the case with the loss curve in the same figure. However, here the values run toward "0".

The confusion matrix in illustrates the good accuracy value on the test data set. Almost all sound samples are classified correctly. However, one sound sample of the "good" class and one sound sample of the "medium" class were each incorrectly assigned to the "poor" class. On the positive side, no sound sample belonging to the "medium" and "poor" classes was assigned to the "good" class. That would be the worst case in practice, but it does not occur here. In so far, the model is working very well.

**Figure 4.** *Confusion Matrix for Complete Sound Samples*

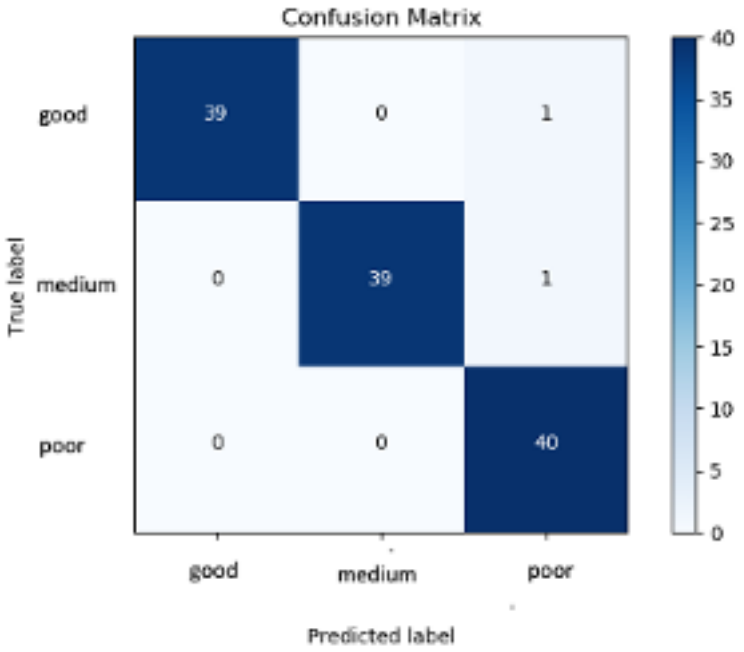

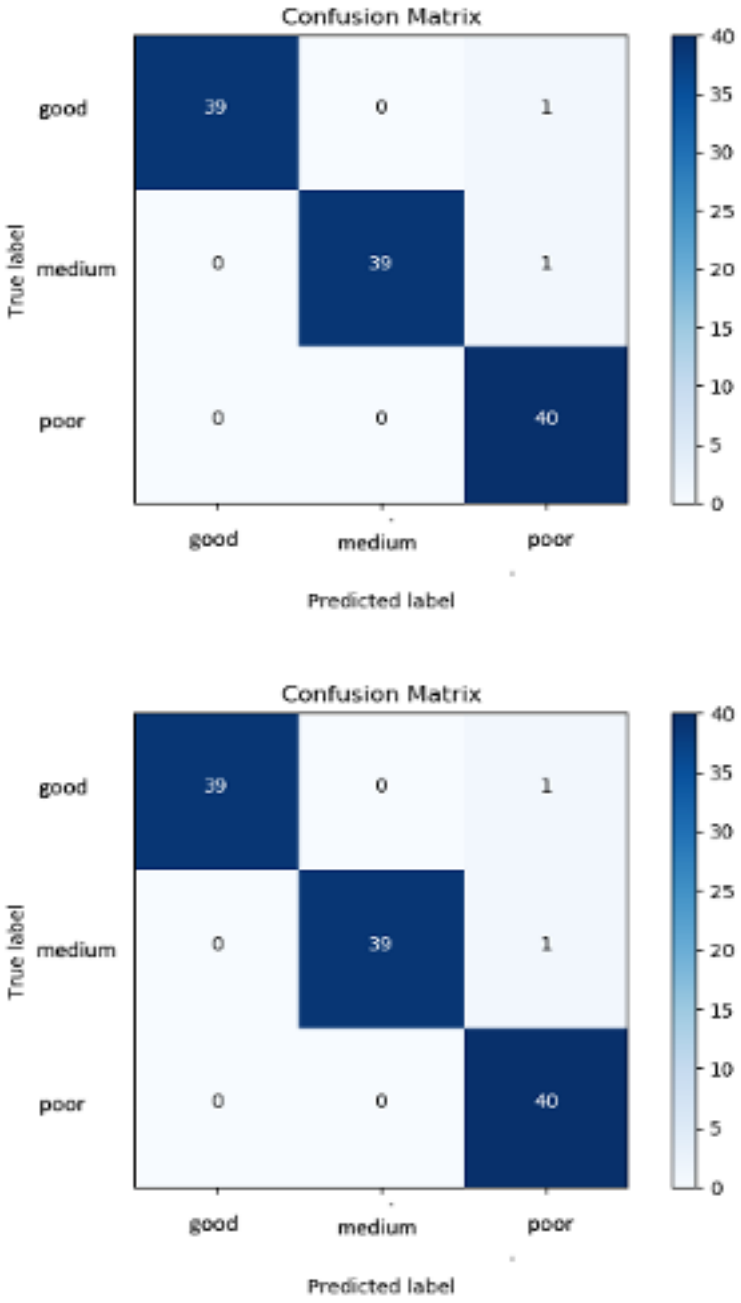


The probability values determined by the model are listed in

Table 4 in the Appendix. Each row in the three tables represents one sound sample. For a more compact overview, the 120 sound samples of the three categories are listed side by side. This results in a total of 40 sound samples per class. The left column indicates the actual category. The three following columns each show the value of the prediction by the model. The values of each category are given in percent.

With this overview, the values of the two incorrectly classified samples can be analyzed. The sample with the actual category "good", is assigned by the model

with 85.13% to the category "poor". Likewise, the sample with the actual group "medium", is assigned by the model with 99.97% to the category "poor". The respective rows are highlighted in the tables.

It is recommended to set a minimum value of at least 80% to ensure an unambiguous classification for all sound samples. Considering this threshold, the result changes from two to six misclassified sound samples. The remaining sound samples are assigned to the correct category by a clear margin.

- Segmented sound samples

The data set is much larger than in the previous method due to the artificial enrichment. This also allows a larger number of learning cycles. As can be seen in Figure 5, a maximum of 60 training cycles are possible with this method until both curves run permanently against a value of "1". This turns out to be optimal for the given test parameters.

Both curves of training and validation run roughly parallel to each other. The validation accuracy curve is slightly worse than the training accuracy curve, which corresponds to a normal curve.

The curve of the loss values, shown in Figure 5, also shows an optimal course of training and validation data. The curves are relatively flat and run almost identically, which does not indicate overfitting or underfitting.

**Figure 5. Model Accuracy and Loss for Semented Sound Samples**

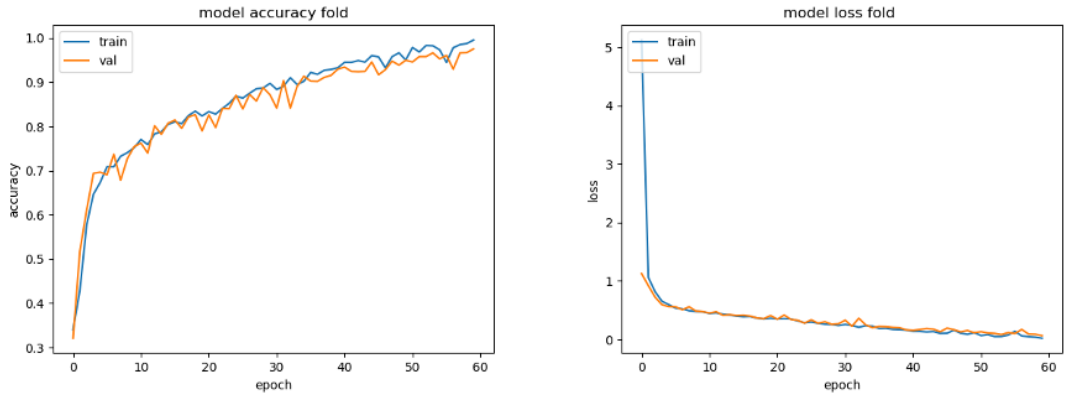


For a smoothed course of the learning cycles of training and validation data, the average values of all models are shown. Here, too, one can see the almost identical course of both values of Accuracy and Loss. The figure shows that there are no major fluctuations among the different models.

Table 3 shows a detailed overview of the individual values of Accuracy and Loss. Each of the ten generated models is listed here.

The achieved accuracy values of the best and worst model hardly deviate from the calculated average of all models. The best model, model no. 5, achieves a value of 90% and the worst model, model no. 7, a value of 86%. The average of all models is 87% accuracy.

As clearly presented in the previous chapter, the probability values in Table 3 are given as percentages. Here, too, each line represents one of the 120 sound samples, which are arranged next to each other by category.

**Table 3.** ***Accuracy and Loss of Each Model***

| Model | Accuracy | Loss |
|---|---|---|
| Model 1 | 0.8833 | 0.4938 |
| Model 2 | 0.8750 | 0.5660 |
| Model 3 | 0.8750 | 0.7467 |
| Model 4 | 0.8667 | 0.5775 |
| Model 5 | 0.9000 | 0.7267 |
| Model 6 | 0.9000 | 0.7494 |
| Model 7 | 0.8625 | 0.8475 |
| Model 8 | 0.8708 | 0.7148 |
| Model 8 | 0.8708 | 0.4842 |
| Model 10 | 0.8708 | 0.3785 |
| Ø | 0.8775 | 0.6285 |

With reference to the results shown in the confusion matrix of Figure 6 the model has difficulties classifying samples of the "good" and "medium" class. Thus, the model, four sound samples of the category "good" with a value of 69.99%, 63.88%, 64.36% and 62.39% are incorrectly assigned to the category "medium". Similarly, three sound samples of the class "good" and one sound sample of the class "poor", are incorrectly assigned to the category "medium". The values for the three sound samples of the category "good" are 67.27%, 74.94% and 68.04% and the value for the single sound sample of the category "poor" is 56.75%.

**Figure 6. Confusion Matrix for Segmented Sound Samples**

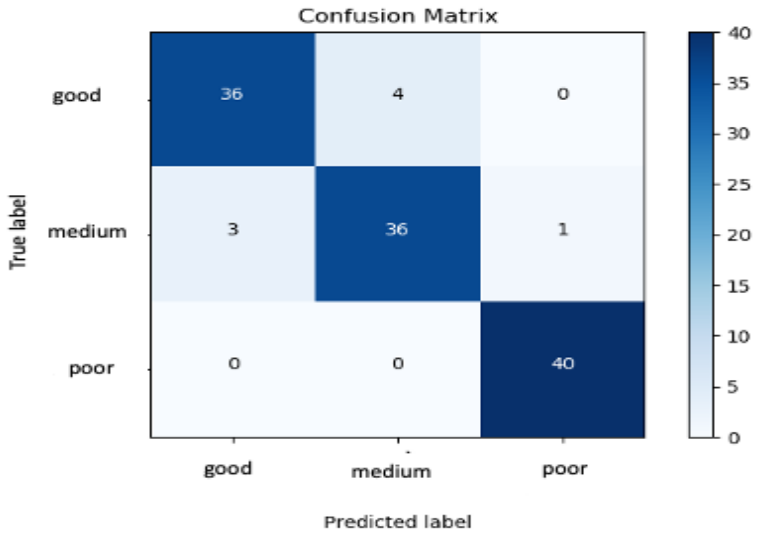

As before with complete sound samples, there are cases that are only categorized with a deviation of 2 to 3% to another class. This should be remedied by a fixed threshold of the probability value of at least 80%. Considering the threshold, the number of misclassified sound samples increases from 8 to 44.

## Discussion

The conducted research shows that quality assurance by means of sound data processing in neural networks leads to very good and usable results, at least in our experimental setup. Regardless the promising results, some crucial points have to be critically pointed out.

The size of 360 sound samples is very small for training neural networks. As shown, the significantly larger number of segmented sound samples - contrary to all expectations - does not lead to better results. This fact requires a more detailed investigation. Regardless of whether "complete" or "segmented" sound samples are used, to substantiate the results obtained so far, the approach should be validated with a significantly larger number of complete sound samples.

Further need for research arises from the fact that the casting parameter were extremely set during the casting process. As already shown, the idea of parameterization was to achieve a defined result. This was undoubtedly achieved in the given laboratory situation: Three disjoint groups of part qualities emerged, which were clearly separable at the data level.

In practice, however, the situation is completely different. The production process is set with the presumably perfect parameters. Over time, it will happen that individual parameters change, for example due to environmental influences or due to variances in the material properties. Defects are thus created insidiously by a minimal variation of several parameters or environmental influences. Accordingly, there are also parts that are "more or less" good. This practically very relevant grey area between the respective classes was not represented by our experiments. In this respect there is a need for further research with significantly less extreme parameter sets.

Furthermore, it must be pointed out that the parts examined here had a very simple geometry, which seems quite appropriate for experimental purposes. In practice, however, the parts are likely to have a much more complex geometry. In this respect, it seems urgent to perform comparable experiments to investigate the effectiveness of the approach for more complex parts.

Regarding the production process in practice, an "inline" solution is conceivable. This would allow the finished parts to be checked for quality within a short time after the casting process. For this purpose, a corresponding testing device should be designed which allows sound samples and their classification to be carried out on a kind of assembly line. Since the sound samples used in this work were generated in the laboratory, further investigations should be carried out in a manufacturing environment. Here, possible interfering noises can occur, which must either be learned beforehand by the model or removed during the preprocessing process.

## Conclusions

The obtained results show that a new inline quality assurance process using sound data processing in neural networks is basically possible. Against the background of the limitations discussed above, it is necessary to conduct further investigations.

## References

Abdoli S, Cardinal P, Lameiras Koerich A (2019) End-to-end environmental sound classification using a 1D convolutional neural network. *Expert Systems with Applications* 136(Dec): 252–263.

Boddapati V, Petef A, Rasmusson J, Lundberg L (2017) Classifying environmental sounds using image recognition networks. *Procedia Computer Science* 112: 2048–2056.

Costa YMG, Oliveira LS, Silla CN (2017) An evaluation of Convolutional Neural Networks for music classification using spectrograms. *Applied Soft Computing* 52(C): 28–38.

Cunha R, Medeiros De Araujo G, Maciel R, Nandi GS, Da-Ros MR, et al. (2018) Applying non-destructive testing and machine learning to ceramic tile quality control. In *SBESC 2018. 2018 VIII Brazilian Symposium on Computing Systems Engineering: Proceedings*, 54–61. Salvador, Brazil, November 6-9, 2018. Los Alamitos, CA: Conference Publishing Services, IEEE Computer Society.

Gulli A (2017) *Deep learning with Keras. Implement neural networks with Keras on Theano and TensorFlow*. Birmingham, UK: Packt Publishing.

Hassan SU, Zeeshan Khan M, Ghani Khan MU, Saleem S (2019) Robust sound classification for surveillance using time frequency audio features. In *2019 International Conference on Communication Technologies (ComTech)*, 13–18. 20-21 March, 2019, Military College of Signals, National University of Sciences & Technology. Piscataway, New Jersey: IEEE.

Huzaifah M (2017) *Comparison of time-frequency representations for environmental sound classification using convolutional neural networks*. Available at: https://arxiv.org/pdf/1706.07156.

Jing L, Zhao M, Li P, Xu X (2017) A convolutional neural network based feature learning and fault diagnosis method for the condition monitoring of gearbox. *Measurement* 111(Dec): 1–10.

Khamparia A, Gupta D, Nguyen NG, Khanna A, Pandey B, Tiwari P (2019) Sound classification using convolutional neural network and tensor deep stacking network. *IEEE Access* 7(Jan): 7717–7727.

Kong Z, Tang B, Deng L, Liu W, Han Y (2020) Condition monitoring of wind turbines based on spatiotemporal fusion of SCADA data by convolutional neural networks and gated recurrent units. *Renewable Energy* 146(Feb): 760–768.

Kothuru A, Nooka SP, Liu R (2019) Application of deep visualization in CNN-based tool condition monitoring for end milling. *Procedia Manufacturing* 34: 995–1004.

Krizhevsky A, Sutskever I, Hinton GE (2017) ImageNet classification with deep convolutional neural networks. *Communications of the ACM* 60(6): 84–90.

Lai J-H, Liu C-L, Chen X, Zhou J, Tan T, Zheng N, et al. (2018) *Pattern Recognition and Computer Vision*. Cham: Springer International Publishing.

Lv N, Xu Y, Li S, Yu X, Chen S (2017) Automated control of welding penetration based on audio sensing technology. *Journal of Materials Processing Technology* 250: 81–98.

Mery D (2020) Aluminum casting inspection using deep learning: a method based on convolutional neural networks. *Journal of Nondestructive Evaluation* 39(1): 1–13.

Moolayil J (2019) *Learn keras for deep neural networks.* Berkeley, CA: Apress.

Nguyen TP, Choi S, Park S-J, Park SH, Yoon J (2020) Inspecting method for defective casting products with convolutional neural network (CNN). *International Journal of Precision Engineering and Manufacturing-Green Technology* 8(Feb): 583–594.

Nie J-Y, Obradovic Z, Suzumura T, Ghosh R, Nambiar R, Wang C (Eds.) (2017) *2017 IEEE International Conference on Big Data. Dec 11-14, 2017, Boston, MA, USA: Proceedings.* Piscataway, NJ: IEEE.

Olson DL, Delen D (2008) *advanced data mining techniques*. Berlin, Heidelberg: Springer-Verlag Berlin Heidelberg.

Piczak KJ (2015) Environmental sound classification with convolutional neural networks. In D Erdoğmuş (ed.), *2015 IEEE 25th International Workshop on Machine Learning for Signal Processing (MLSP*), 1–6. 17-20 Sept. 2015, Boston, USA. Piscataway, NJ: IEEE.

Przybył K, Duda A, Koszela K, Stangierski J, Polarczyk M, Gierz L (2020) Classification of Dried Strawberry by the Analysis of the Acoustic Sound with Artificial Neural Networks. *Sensors (Basel, Switzerland)* 20(2): 499.

Purwins H, Li B, Virtanen T, Schluter J, Chang S-Y, Sainath T (2019) Deep learning for audio signal processing. *IEEE Journal of Selected Topics in Signal Processing* 13(2): 206–219.

Salamon J, Bello JP (2017) Deep convolutional neural networks and data augmentation for environmental sound classification. *IEEE Signal Processing Letters* 24(3): 279–283.

Simonyan K, Zisserman A (2014) *Very deep convolutional networks for large-scale image recognition. https://arxiv*.org/pdf/1409.1556

Voith (2020) *OnCare.* Available at: http://voith.com/corp-de/products-services/automatio n-digit al-solutions/oncare.html?

Wani MA, Bhat FA, Afzal S, Khan AI (2020) *Advances in deep learning.* Singapore: Springer.

Yuji Tokozume TH (2017) *Learning environmental sounds with end-to-end convolutional neural network.* IEEE.

## Appendix

**Table 4.** *Probability Values for All Complete Sound Samples*

| | class | | |
|---|---|---|---|
| **good** | | **medium** | **poor** |
| **good** | 99,97 | 0,03 | 0,00 |
| **good** | 92,62 | 7,38 | 0,00 |
| **good** | 91,79 | 7,95 | 0,26 |
| **good** | 83,11 | 16,87 | 0,02 |
| **good** | 67,24 | 32,73 | 0,03 |
| **good** | 94,76 | 4,94 | 0,31 |
| **good** | **14,79** | **0,09** | **85,13** |
| **good** | 79,21 | 20,77 | 0,02 |
| **good** | 97,58 | 2,40 | 0,02 |
| **good** | 97,25 | 2,72 | 0,03 |
| **good** | 99,84 | 0,11 | 0,05 |
| **good** | 99,13 | 0,86 | 0,01 |
| **good** | 99,77 | 0,19 | 0,03 |
| **good** | 99,71 | 0,29 | 0,01 |
| **good** | 99,68 | 0,30 | 0,02 |
| **good** | 99,99 | 0,01 | 0,00 |
| **good** | 99,90 | 0,10 | 0,00 |
| **good** | 98,99 | 1,00 | 0,00 |
| **good** | 99,95 | 0,05 | 0,00 |
| **good** | 99,88 | 0,12 | 0,00 |
| **good** | 99,72 | 0,28 | 0,00 |
| **good** | 85,79 | 1,53 | 12,69 |
| **good** | 100 | 0,00 | 0,00 |
| **good** | 98,00 | 1,99 | 0,01 |
| **good** | 99,85 | 0,10 | 0,05 |
| **good** | 81,28 | 18,69 | 0,03 |
| **good** | 99,99 | 0,01 | 0,01 |
| **good** | 99,90 | 0,06 | 0,04 |
| **good** | 95,47 | 4,43 | 0,10 |
| **good** | 99,31 | 0,68 | 0,01 |
| **good** | 91,44 | 8,54 | 0,02 |
| **good** | 82,90 | 16,99 | 0,11 |
| **good** | 99,90 | 0,10 | 0,00 |
| **good** | 99,85 | 0,09 | 0,06 |

| | class | | |
|---|---|---|---|
| **good** | | **medium** | **poor** |
| **medium** | 37,96 | 56,25 | 5,80 |
| **medium** | 7,10 | 90,67 | 2,23 |
| **medium** | 32,53 | 67,35 | 0,12 |
| **medium** | 3,71 | 96,28 | 0,01 |
| **medium** | 0,03 | 99,97 | 0,00 |
| **medium** | 0,01 | 99,99 | 0,00 |
| **medium** | 0,00 | 100,00 | 0,00 |
| **medium** | 0,00 | 100,00 | 0,00 |
| **medium** | 0,13 | 99,86 | 0,01 |
| **medium** | 0,07 | 99,93 | 0,01 |
| **medium** | 0,27 | 99,72 | 0,01 |
| **medium** | 0,00 | 100,00 | 0,00 |
| **medium** | 0,00 | 100,00 | 0,00 |
| **medium** | 0,00 | 100,00 | 0,00 |
| **medium** | 0,00 | 100,00 | 0,00 |
| **medium** | 0,00 | 100,00 | 0,00 |
| **medium** | 0,00 | 100,00 | 0,00 |
| **medium** | 0,11 | 99,89 | 0,01 |
| **medium** | 0,79 | 98,94 | 0,28 |
| **medium** | 0,06 | 99,94 | 0,00 |
| **medium l** | 0,41 | 99,57 | 0,02 |
| **medium** | 0,02 | 99,98 | 0,00 |
| **medium** | 7,75 | 92,22 | 0,04 |
| **medium** | **0,03** | **0,00** | **99,97** |
| **medium** | 0,44 | 99,56 | 0,00 |
| **medium** | 0,00 | 100,00 | 0,00 |
| **medium** | 1,73 | 97,94 | 0,33 |
| **medium** | 0,00 | 100,00 | 0,00 |
| **medium** | 0,00 | 100,00 | 0,00 |
| **medium** | 0,00 | 100,00 | 0,00 |
| **medium** | 0,00 | 100,00 | 0,00 |
| **medium** | 0,03 | 99,94 | 0,03 |
| **medium** | 0,00 | 99,99 | 0,00 |

| | class | | |
|---|---|---|---|
| **good** | | **medium** | **poor** |
| **poor** | 0,27 | 0,00 | 99,73 |
| **poor** | 0,07 | 0,00 | 99,93 |
| **poor** | 0,25 | 0,01 | 99,75 |
| **poor** | 0,36 | 0,01 | 99,63 |
| **poor** | 0,10 | 0,00 | 99,90 |
| **poor** | 0,51 | 0,00 | 99,49 |
| **poor** | 0,50 | 0,00 | 99,50 |
| **poor** | 1,71 | 0,01 | 98,28 |
| **poor** | 4,07 | 0,08 | 95,86 |
| **poor** | 0,14 | 0,00 | 99,86 |
| **poor** | 0,06 | 0,00 | 99,94 |
| **poor** | 0,00 | 0,00 | 100,00 |
| **poor** | 0,01 | 0,00 | 99,99 |
| **poor** | 0,00 | 0,00 | 100,00 |
| **poor** | 0,00 | 0,00 | 100,00 |
| **poor** | 0,05 | 0,00 | 99,95 |
| **poor** | 0,25 | 0,00 | 99,75 |
| **poor** | 1,30 | 0,03 | 98,67 |
| **poor** | 0,00 | 0,00 | 100,00 |
| **poor** | 0,03 | 0,00 | 99,97 |
| **poor** | 0,03 | 0,00 | 99,97 |
| **poor** | 0,04 | 0,00 | 99,96 |
| **poor** | 0,00 | 0,00 | 100,00 |
| **poor** | 0,00 | 0,00 | 100,00 |
| **poor** | 0,05 | 0,00 | 99,95 |
| **poor** | 0,00 | 0,00 | 100,00 |
| **poor** | 0,02 | 0,00 | 99,98 |
| **poor** | 0,01 | 0,00 | 99,99 |
| **poor** | 0,00 | 0,00 | 100,00 |
| **poor** | 0,01 | 0,00 | 100,00 |
| **poor** | 0,02 | 0,00 | 99,98 |
| **poor** | 0,02 | 0,00 | 99,98 |
| **poor** | 0,04 | 0,00 | 99,96 |
| **poor** | 0,00 | 0,00 | 100,00 |
| **poor** | 0,14 | 0,00 | 99,86 |
| **poor** | 0,09 | 0,00 | 99,91 |
| **poor** | 0,10 | 0,00 | 99,90 |
| **poor** | 0,02 | 0,00 | 99,98 |

*Athens Journal of Sciences- Volume 11, Issue 1, March 2024 – Pages 29-38*

# Proof of Principle of Wastewater Treatment using Plasma Discharge to Reduce the Amount of Methylparaben

*By Christoph Schattschneider[*], Sina Piontek[±], Hannes Jacobs[°], Andrea Böhme[•], Concetta Sirena[♦] & Andreas Foitzik[♥]*

*Synthetic substances like many pharmaceuticals, preservatives or other chemical compounds are actually very difficult to handle in sewage treatment. These compounds are very stable in aqueous solution and their degradation reactions are insufficient. Therefore, to eliminate these substances from wastewater additional afford is necessary. Extreme conditions like pH value, redox potential, chemical or physical energy need to be present. With our study we try to show that the use of plasma discharge could be a solution to this problem. Using the example of methylparaben, a preservative, we could show, that the physical energy of plasma discharge is able to initialize the degradation reaction in aqueous environment. The concentration was reduced by up to 70 percent in our setting depending on the treatment duration. Overall, the system showed potential to optimize wastewater treatment. Further examinations are necessary for example regarding undesirable by-products.*

**Keywords:** *wastewater treatment, plasma discharge, high voltage, degradation*

## Introduction

Wastewater treatment generally takes place in three stages. The first treatment stage is the mechanical treatment, which consists of pre-treatment and primary treatment (Sonune and Ghate 2004). The second stage of treatment is the biological treatment, for which there are three common processes: the activated sludge process, the biofilm process, and the near-natural process (Resch and Schatz 2020). The standard is the activated sludge method with a total of around 99% of the wastewater connected to the system throughout Germany being treated using biological methods (Umwelt Bundesamt 2021). Chemical purification serves as the third purification stage, whereby precipitants and flocculants can be used to remove phosphorus, for example.

In 2016, approximately 9.6 billion cubic meters of wastewater were treated in 9105 public wastewater treatment plants across Germany (Statistisches Bundesamt - Destatis 2018). Here, 97% of the German population is connected to the public sewage system [Statistisches Bundesamt - Destatis (2018)]. Especially biological

[*]PhD-Student, Tor Vergata University of Rome, Italy.
[±]Graduate Student, Berlin University of Applied Sciences and Technology, Germany.
[°]Scientific Assistant, Technical University of Applied Sciences Wildau, Germany.
[•]Scientific Assistant, Technical University of Applied Sciences Wildau, Germany.
[♦]Scientific Assistant, Tor Vergata University of Rome, Italy.
[♥]Professor, Technical University of Applied Sciences Wildau, Germany.

and chemical contamination and pollution have increased in the last 30 years and represent a major environmental problem (Crini andLichtfouse 2018).

It has been clear for some time that trace substances often cannot be completely removed from wastewater if the wastewater treatment plant only has a mechanical and biological treatment stage Clara et al. 2002). The term "trace substances" refers to all substances foreign to nature that occur in wastewater in millionths or billionths of a gram per liter (Metzger et al. 2012), and this can be numerous, as more than 100,000 products foreign to nature are distributed throughout Europe (as of 2018) (Eberlein et al. 2018). These products sooner or later enter the environment and accumulate in the water (Eberlein et al. 2018). To minimize the discharge of trace substances into water bodies and the environment, wastewater treatment plants, which represent the main input pathway for organic, anthropogenic trace substances (Benstom 2017), are to be retrofitted with a fourth treatment step. At present, this mostly consists of adsorption on activated carbon or ozonation since both the cleaning performance and the economic efficiency are achieved with these methods (Metzger et al. 2019). The general cost of wastewater treatment by ozonation ranges from 0.03-0.12 €/$m^3$ and that of wastewater treatment with powdered activated carbon from 0.05-0.10 €/$m^3$ (Resch and Schatz 2020).

The use of plasma in water treatment is not completely unknown, though still in the early stages of development (Cui et al. 2018). Plasma is referred to as a fourth state of matter. It is defined as matter with a sufficiently high proportion of ions and electrons and is created when gas is ionized by an energy input, although the definition does not exclude liquids as well (Stroth 2018). Plasma is considered to be an advanced oxidant, and when reacting with water, hydrogen radicals are formed, which are considered to be highly reactive. Ozone is also formed, which again leads to radical formation and further oxidation reactions. In addition, the formation of hydrogen peroxide can occur, as well as further radical formation through the so-called silent electrical discharge of the plasma. This makes the entire system highly reactive (Cui et al. 2018).

In the plant used, a similarly reactive environment is created by the interaction of cavitation, plasma with radical formation, UV radiation, shock waves, and charged particles, which has already been successfully tested in a previous pilot plant (Abramov et al. 2021).

The research objective of the work was to investigate whether this plant is able to break down chemical compounds in water. This is a conceptual proof, for which methylparaben was chosen as a model molecule. Methylparaben finds its application as a preservative in shampoos and other cosmetics, as well as in liquid pharmaceuticals and in research in bacterial agar plates to prevent fungal infestation (Fiedler and Haufe 2010). It was to be determined to what extent the methylparaben can be disintegrated by the plant, whether undesirable by-products occur, and how economical the plant is at this point in time.

## Experimental

Figure 1 shows a scheme of the plant used. The plant used for the tests is larger than the first pilot plant that was developed (Abramov et al. 2021), but has less measuring equipment and a copper electrode instead of a silver electrode. The connected external pump can bring the liquid to a maximum pressure of 250 bar. From there, the sample passes through a nozzle into the reaction chamber, where it meets the plasma. The device has a power supply that is connected to an external transformer. The resulting high voltage can be regulated in a range from 10 to 24 kV alternating current. The frequency can be varied between 30 and 45 kHz. The transformer is attached to the two copper electrodes, at the two ends of the reaction chamber. Frequency and voltage can be adjusted by rotary controls. When the ratio, which can vary depending on the experimental condition such as temperature of the sample, is correct, the plasma ignites. At a pressure of 80 bar, which was used during the experiments, up to 960 L/h can be passed over the plasma once with the aid of the application.

**Figure 7.** *Schematic Structure of the Plasma Generating Plant*

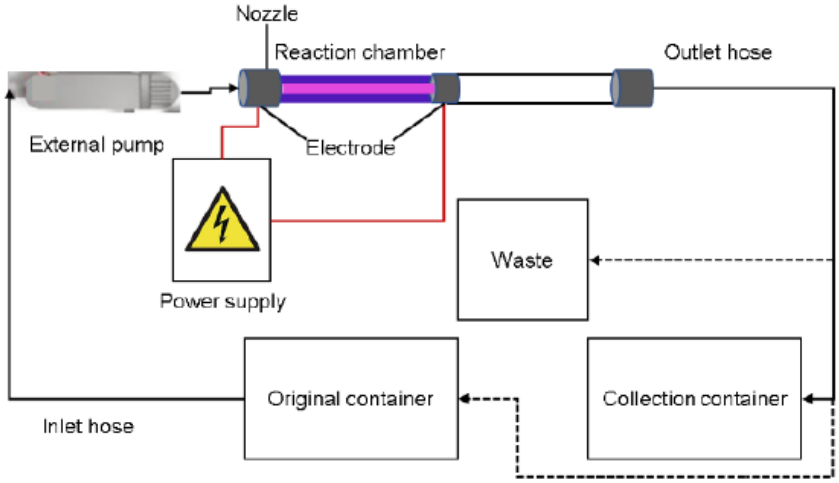


For the methylparaben treatment, 20 L of a 1000 mg/L methylparaben demineralized water solution was prepared. This solution was circulated through the system three times, with sampling after each run. The 20 L batch of sample was then cycled through the system continuously for 5 minutes and finally for an additional 5 minutes, resulting in a maximum treatment time of 3 cycles + 10 minutes. A pressure of 80 bar was used and both voltage and frequency had to be constantly readjusted, so that no clear parameters could be established. However, since this is a prototype and the initial aim is to provide conceptual proof of the functionality, the determination of specific parameters was not the goal of the experiment for the time being.

During the plasma treatment of the samples, the light spectrum generated by the plasma was measured with the aid of a spectrometer (Ocean Optics Inc., Spectrometer USB2000+).

For HPLC analysis, 2 mL of sample was filtered (0.2 µm Phenomenex Inc.) and placed in HPLC sample vials. The tubes were then placed in the system (capillary LC system series 1100; column: ZORBAX Eclipse Plus C18 4.6 x 100; 3.5 mm). A flow rate of 1.2 mL/min and a temperature of 40 °C were used. A methanol-water mixture (composition 1:1) served as the mobile phase, detection was performed by a UV/VIS detector at 254 nm, and 5 µL of sample was injected in each case.

For gas chromatography, the sample was also filtered (0.2 µm Phenomenex Inc.), placed in the proper slots, and the gas chromatography (GCMS-QP2010 SE) was started. 6 µL of sample were injected and heated to 250 °C. A split ratio of 1:10 was used and helium served as the mobile phase. Detection and identification were performed using the mass-specific detector, which was coupled to the "NIST" database.

## Results

Figure 2 shows the plasma generated during the experiment, which was characterized by a pinkish-purple color. During the experiment, there were temporary dropouts of the plasma which required a readjustment of the voltage and frequency. The light emission from the plasma was measured spectroscopically and shown in Figure 3, where several peaks were observed.

**Figure 8.** *Section of the System with the Plasma Generated during Sample Treatment*

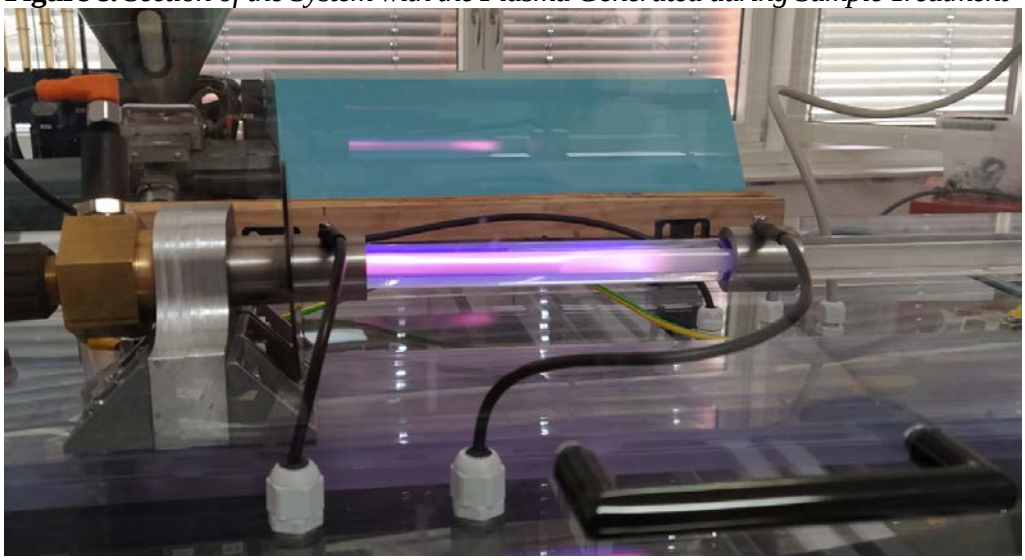

During treatment, discoloration of the samples to a brownish color occurred. This discoloration intensified with increasing treatment time.

**Figure 9.** *Recorded Light Spectrum of the Plasma. The Spectrum was recorded Several Times during the On-Phase of the Plasma*

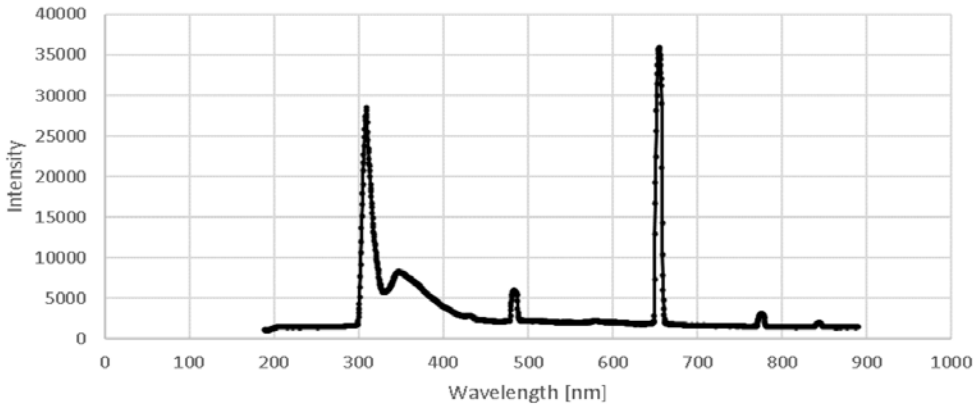


In the HPLC analysis of the plasma-treated methylparaben samples, a major peak was detected in each sample. As can be seen in Figure 4, this peak, which was between a retention time of 1.8 min and 2 min, declined with increasing treatment time. In addition, other small peaks between 0.5 min and 1.5 min retention time could be detected in the treated samples, which were not present in the untreated sample. At the highest treatment duration, the total area reduction was over 70%.

**Figure 10.** *HPLC Chromatograms of the Methylparaben Samples. The Absorbtion Intensity was plotted against the Retention Time of Each Sample in Single Determination*

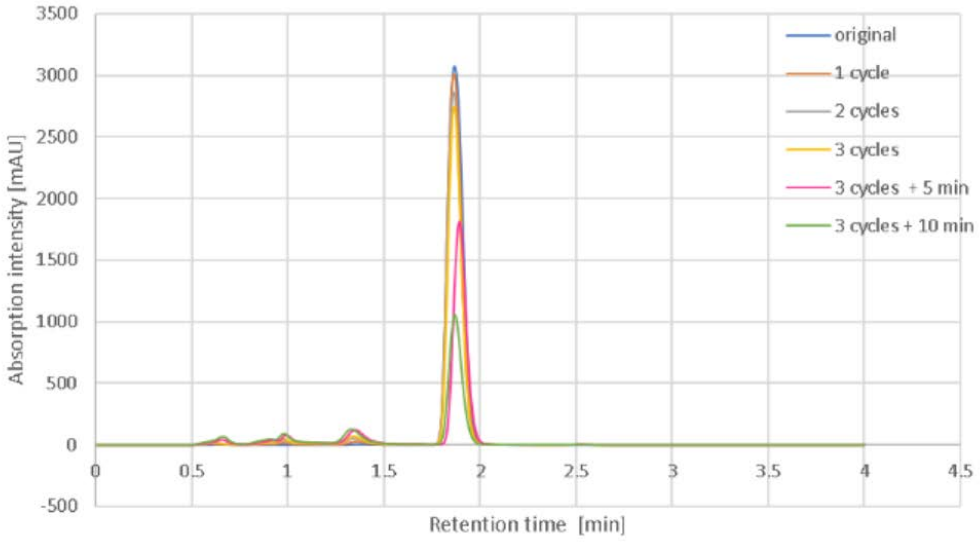


GC-MS of all methylparaben samples detected one large peak each and identified it as methylparaben. This peak was declining with rising treatment time, which can be seen in Figure 5. Additional peaks were only visible when the baseline was examined more closely. Not all peaks could be identified. Among the top emerging compounds that could be allocated were guaiacol and methyl

protocatechuate. The highest number of newly formed peaks was found in the sample with the longest treatment time and amounted to 26 new detected peaks of which 19 could be identified.

Despite the appearance of new peaks, the total area of all peaks combined dropped significantly, reaching an overall reduction of over 50% at the highest treatment duration, which was only 12% less than the change in the methylparaben peak. It can be concluded that methylparaben was not completely converted to by-products. Total peak decrease and methylparaben peak decrease are shown in Figure 6.

**Figure 11.** *During GC-MS of Methylparaben Determined Areas of Methylparaben Peaks, Total Peak Areas and the Differential*

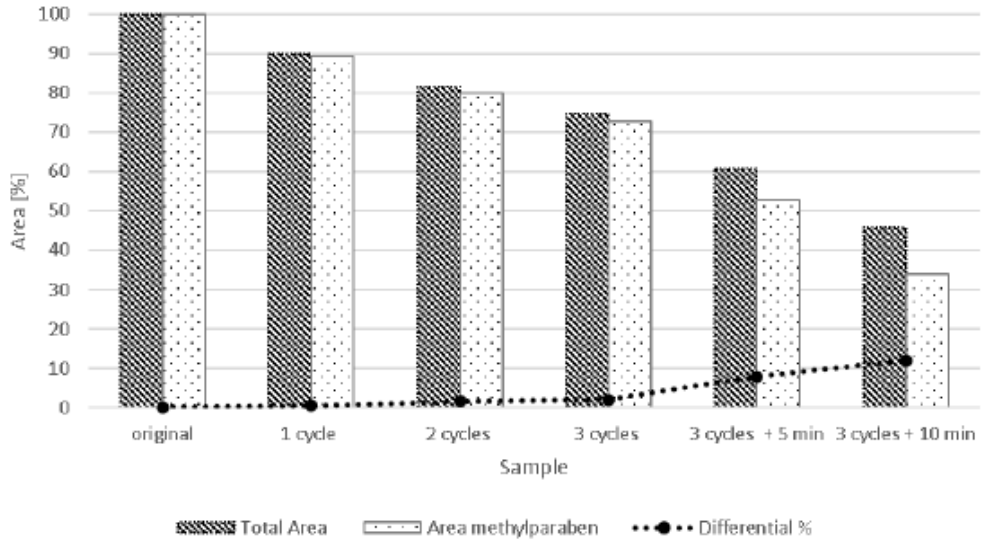


## Discussion

Both the HPLC and GC-MS results demonstrated that degradation of methylparaben occurred, although by-products were formed in the process. The GS-MS results indicated that the methylparaben was completely decomposed to a certain extent, with carbon dioxide and water as the presumed end products. The decomposition presumably takes place here due to the highly reactive environment and the strong radical formation (Cui et al. 2018, Abramov et al. 2021, Bang et al. 2019). However, even with the longest treatment period, elimination was not even close to 100%. The reduction was nevertheless in the competitive range for ozonation. Depending on the pH value and the intensity of ozonation, reductions of 34% to 90% can be achieved with a 10-minute treatment period (Dona et al. 2019).

**Figure 12.** *Comparison of the Peaks after Gas Chromatography with Coupled Mass Spectrometry for the Aqueous Samples*

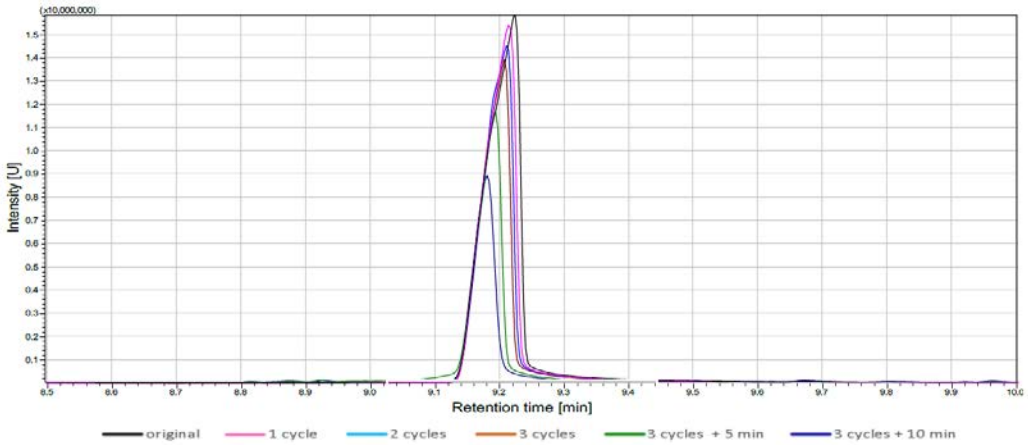


Unwanted by-products could be detected and should be avoided. For example, the identified guaiacol can react in wastewater with nitrogen dioxide present to form nitroguaiacol and 2-methoxybenzene-1,4-diol, which have a higher toxicity than guaiacol itself (An et al. 2019). However, guaiacol is also not without hazard and exhibits acute toxicity to mice (Martinez et al. 2009). Methyl protocatechuate, on the other hand, shows no significant toxic properties, showing evidence of prolonging the life of the nematode Caenorhabditis elegans (Zhang et al. 2014) and exhibits neuroprotective effects in the disease retinitis pigmentosa in mice (Zhang et al. 2017). Hydroquinone was also detected in lower amounts but kept increasing with the duration of treatment. Hydroquinone exhibits elevated levels of toxicity to microorganisms in the soil (Chen et al. 2009). Accordingly, the input into ecological systems should be avoided.

The prototype shows potential for further development and possible improvements. Particular attention should be paid to the efficiency of the application, an extension of the instrumentation, and an automated control of the system. These requirements were concluded for the following reasons. In terms of efficiency, the plant cannot compete at present with the already established methods like ozonation and adsorption on activated carbon (Metzger et al. 2012). Especially in terms of energy efficiency, there is a big potential for improvement. With a total energy consumption by the prototype of approx. 13.3 kWh, the price of a single cycle treatment would be over 1 €/m3 (Considering the average electricity price of 0.3263 €/kWh in Germany in 2021 (Umwelt Bundesamt 2021)), however, parts of the consumption are also due to external pumps and here lies a potential for cost savings. The use of oxidizing agents, such as hydrogen peroxide, would also be conceivable (Bang et al. 2019), to heighten the efficiency and reduce the number of cycles needed. An extension of the monitoring equipment for an actual industrial plant would also make sense in order to be able to ensure a constant plasma intensity. In this process, a possible automation of the plant is also recommended to reduce manual readjustments and therefore reduce staff deployment. The occurrence of the undesirable by-products should be kept as low as possible. However, this problem is not a new one in wastewater treatment

and also occurs with ozonation (Statistisches Bundesamt - Destatis 2018). Here, a post-treatment, for example in the form of rapid filtration, may be selected in order to remove the unwanted components (Crini and Lichtfouse 2018). Overall, the pilot plant displayed potential to be further developed into an industrial plant.

## References

Abramov VO, AbramovA AV, Cravotto G, Nikonov RV, Fedulov IS, Ivanov VK (2021) Flow-mode water treatment under simultaneous hydrodynamic cavitation and plasma. *Ultrason Sonochem* 70(Jan): 105323.

An Z, Sun J, Han D, Mei Q, Wei B, Wang X, et al. (2019) Theoretical study on the mechanisms, kinetics and ecotoxicity assessment of OH-initiated reactions of guaiacol in atmosphere and wastewater. *Science of the Total Environment* 685(Oct): 729–740.

Bang HJ, Lee H, Park Y-K, Ha H-H, Yu YH, Kim B-J, et al. (2019) Assessment of degradation behavior for acetylsalicylic acid using a plasma in liquid process. *Catalysts* 9(11): 965–975.

Benstom F (2017) *Granulierte Aktivkohle zur Elimination organischer Spurenstoffe aus kommunalem Abwasser*. (Granulated activated carbon for eliminating organic trace substances from municipal wastewater.) Aachen.

Chen H, Yao J, Wang F, Choi MMF, Bramanti E, Zaray G (2009) Study on the toxic effects of diphenol compounds on soil microbial activity by a combination of methods. *Journal of Hazardous Materials* 167(3): 846–851.

Clara M, et al. (2002) *Verhalten ausgewahlter Pharmazeutika in der Abwasserreinigung.* (Behavior of selected pharmaceuticals in wastewater treatment, in pharmaceuticals in the aquatic environment.) In *Arzneimittel in der aquatischen Umwelt*, volume 178. Wien: Wiener Mitteilungen.

Crini G, Lichtfouse E (2018) Advantages and disadvantages of techniques used for wastewater treatment. *Environmental Chemistry Letters* 17(Jul): 145–155.

Cui Y, Cheng J, Chen Q, Yin Z (2018) The types of plasma reactors in wastewater treatment. *IOP Conference Series Earth and Environmental Science* 208(1):012002.

Dona G, et al. (2019) Efficient remove methylparaben by ozonation process. *International Journal of Environmental Science and Technology* 16(5): 2441–2454.

Eberlein J, et al. (2018) *Spurenstoffe und antibiotikaresistente Bakterien-Schnittstelle Abwasserent-und Wasserversorgung - Stuttgarter Berichte zur Siedlungswasserwirtschaft Band 242*. (Trace substances and antibiotic-resistant bacteria interface sewage disposal and water supply - Stuttgart reports on urban water management Volume 242.) Stuttgart.

Fiedler D, Haufe H (2010) *Klimastabile Verpackungsmaterialien durch antimikrobielle Nanosol-Beschichtungen.* (Climate-stable packaging materials thanks to antimicrobial nanosol coatings.)

Martinez EME, Del Villar A, Chauvet D, Lopez Valle A, Susano Pompeyo M, Campos Sepulveda AE (2009) Acute toxicity of guaiacol administered subcutaneously in the mouse. *Proceedings of the Western Pharmacology Society* 52: 92–93.

Metzger S, et al. (2012) *Erweiterung des Klarwerks Mannheim um eine Adsorptionsstufe zur Verbesserung der Abwasserreinigung*. (Expansion of the Mannheim wastewater treatment plant to include an adsorption stage to improve wastewater treatment.) Biberach.

Metzger S. et al. (2019) *Aktivkohleeinsatz auf kommunalen Kläranlagen zur Spurenstoffentfernung - Verfahrensvarianten, Reinigungsleistung und betriebliche Aspekte -, T1 ed., vol. DWA-Themen*. (Use of activated carbon in municipal sewage treatment plants for the removal of trace substances - process variants, cleaning performance and operational aspects -, T1 ed., vol. DWA topics.) Hennef: Deutsche Vereinigung fur Wasserwirtschaft, Abwasser und Abfall.

Resch H, Schatz R (2020) *Abwassertechnik verstehen Ein kleines 1 x 1 der Abwassertechnik für Einsteiger und Laien*. (Understanding wastewater technology A small 1 x 1 of wastewater technology for beginners and laypeople.) 2nd Edition. Hennef: DWA.

Sonune A, Ghate R (2004) Developments in wastewater treatment methods. *Desalination* 167: 55–63.

Statistisches Bundesamt - Destatis (2018) Offentliche Wasserversorgung und offentliche Abwasserentsorgung - Offentliche Wasserversorgung – 2016. (Public water supply and public sanitation - Public water supply – 2016.) Fachserie 19 Reihe 2.1.2, 20–22.

Stroth U (2018) *Plasmaphysik Phanomene, Grundlagen und Anwendungen*. (Plasma physics phenomena, basics and applications.) 2nd Edition. Berlin, Heidelberg: Springer Spektrum.

Umwelt Bundesamt (2021, February 9) *Offentliche Abwasserentsorgung*. (Public wastewater disposal.) Available at: https://www.umweltbundesamt.de/daten/wasser/wasserwirtschaft/oeffentliche-abwasserentsorgung.

Zhang W, Cai L, Geng H-J, Su C-F, Yan L, Wang J-H, et al. (2014) Methyl 3,4-dihydroxybenzoate extends the lifespan of Caenorhabditis elegans, partly via W06A7.4 gene. *Experimental Gerontology* 60(Dec): 108–116.

Zhang J, Xu D, Quyang H, Hu S, Li A, Luo H, et al. (2017) Neuroprotective effects of methyl 3,4 dihydroxybenzoate in a mouse model of retinitis pigmentosa. *Experimental Eye Research* 162(Sep): 86–96.

*Athens Journal of Sciences- Volume 11, Issue 1, March 2024 – Pages 39-54*

# Algorithm for Control of Traffic Flow in an Intelligent Transport System

*By Natallia Yankevich*[*]

*Traffic management in modern Intelligent Transport Systems (ITS) includes monitoring the actual traffic situation in real time and management transport traffic using this information. At the same time, cars as ITS components must be equipped with communication capabilities for exchanging information with other vehicles (V2V) and road infrastructure (V2I). Such approach is connected with usage of special equipment connected to on-board network for local data collection, which can be exchanged between cars and with a central communication station using wireless Internet. At the same time, the issue of developing the traffic organization algorithms themselves is still open. This problem can be solved with the help of game theory, a fairly new but rapidly developing part of modern mathematics. Unlike optimization theory, which studies the possibilities of constructing an optimal solution for the entire system as a whole, game theory studies ways to optimize individual benefits in competition with other persons (events) that rationally seek to satisfy their own benefits. The problem of "smart" regulation of intersections is quite difficult to solve a problem, nevertheless it is possible due to rapid development of ICT technologies.*

**Keywords:** *ITS, transport crossroads, game theory*

## Introduction

Modern technologies, making it possible to improve traffic control in real time and increase its environmental friendliness, are the basis for the introduction of new services. In addition to the obvious benefits for transport operators and customers, new logistics systems (in particular intelligent transport systems) will provide public administration with operational information, including data on infrastructure and maintenance needs.

The development of an open architecture will ensure interoperability and flexible development of various applications for future modes of transport. The structure of such an automated traffic control system using modern communication and information technologies is invariant as technologically universal, since it has continuity in the interface protocols with existing automated traffic control systems due to the openness of their system architectures.

The described “intellectualization” approach significantly expands the range of capabilities of such systems and provides:

[*]Head of the Department, SSI "Center for the System Analysis and Strategic Research of the National Academy of Sciences of Belarus", Republic of Belarus.

- implementation of programs for the continuous movement of vehicles through intersections along avenues and city streets through special coordination plans that synchronize shifts in the cyclic phases of vehicle movement through system controllers;
- receiving signals from the regulated object ("smart" controllers) for further analysis;
- dispatch control – functions for calling stages, subroutines, special flights and control with deferred execution;
- geographic monitoring on an electronic map of the city with the implementation of a visualization function.

The main prospects for the further creation of traffic control automation tools are currently associated with new technologies in the development of modern road controllers, as well as innovative reliable operational communication between them and the Data Processing Center (DPC). The structure of such an automated traffic control system using modern communication and information technologies is invariant as a technological universal, since it has continuity in the interface protocols with existing automated traffic control systems due to their openness.

The practical implementation of these approaches is based on modern communication technologies that provide data transfer between cars - V2V (Vehicle-to-Vehicle) or between cars and road infrastructure - V2I (Vehicle-to-Infrastructure) and based on wireless communication standards DSRC (Dedicated short- range communications), WAVE (Wireless Access in Vehicular Environments) IEEE 802.11p (Hiertz 2010). One application of these technologies is to improve traffic control algorithms to increase the capacity of transport networks.

The general principle of management of transport traffic at an intersection using V2I interaction, as a rule, is to install at the intersection a special transmitter device (RSU - road side unit) connected via a wired (or wireless) connection to a server or local traffic control center (DPC). The transmitter has a certain range of action, within which cars are able to exchange data with it, reporting their position, speed and route. Based on the collected information, in accordance with the control algorithm, the system generates commands for cars that control the order of passage of the intersection, the efficient and safe use of its capacity.

The creation and operation of V2I and V2V systems requires significant funds and is rational only if there is a relatively large coverage of most of the transport system (otherwise the system will not be in demand, and equipment manufacturers will not be able to compensate the costs for its development). Therefore, the need to implement ITS within large-scale projects serves as a significant brake on their development.

In addition, the principles for standardizing traffic information have not yet been fully developed. The greatest amount of work has been done in the area of standardization of infrastructure-to-user communications (i.e., I2V).

At the same time, there are a number of other problems associated with the development of ITS components, for example, in terms of navigation:

- data filtering in the vehicle unit, which will significantly reduce the amount of data transmitted by the vehicle unit to the control center;
- the possibility of using several GNSS systems, and, consequently, various types of signals and structures that have not been tested on a large scale. It is expected that errors associated with multipath transmission of information will be significantly reduced and that the availability of satellite information will be improved, especially in urban areas.

However, the main problem with this approach is that all these components and methodologies are not integrated and therefore cannot provide real-time information to the user. A centralized database for an intelligent traffic control system on a large scale is too slow to provide real-time results. In addition, GPS navigators (Tom-Tom, Garmin) have mostly unidirectional communication channels. Vehicles that are equipped with in-vehicle data communication technologies are rare, and they cannot provide a central communications station database on a sufficient scale.

A key requirement for real-time traffic control systems to generate meaningful contextual information from the analysis of incoming data is high quality. In this case, "quality" is determined by three criteria:

- accuracy;
- completeness;
- timeliness.

Traditionally, the "relevance" parameter has not received much attention, as analysis has focused primarily on processing static data with low time deviations. With the advent of various real-time data sources (cameras, GPS sensors, mobile phones, traffic light controllers, etc.) and the creation of new paradigms of real-time sensor applications (situational awareness), the relevance of the database is now rapidly gaining importance. Thus, a mechanism must be created to integrate sensor measurements and other data in real time, which combines various data sources obtained using standard interfaces.

In addition to standardized data transmission and processing, special attention must be paid to the issue of functional processing of complex events (Complex Event Proceeding - CEP) by spatial components. Because the information content of this contextual knowledge is of higher quality than that of the original raw data, the business decisions that flow from it can be more accurate. However, these approaches are not yet sufficiently developed and require further development.

The implementation of these new approaches requires the development of systems based on CEP, with a clear description of algorithms for processing measurement data and rules for resolving complex events, respectively (time, space, parameters of measurements, etc.).

A big step forward in this direction has been "intelligent" cooperative systems (ICTS). ICTSs based on vehicle-to-vehicle (V2V) and vehicle-to-infrastructure (V2I) communications promise significant improvements in both the efficiency of transport systems and the safety of all road users. The goal of ICTS

solutions is to provide assistance while driving, taking into account the early detection of emerging emergency events. This is achieved through a communications-based system that empowers drivers by keeping them well and reliably informed about the environment, other vehicles and driving conditions, and makes it possible to alert the driver in a timely manner to potentially dangerous situations.

The problem of "intelligent" regulation of the intersections is a rather difficult task for solution of which it is necessary to combine the efforts of scientists from different fields of knowledge. However, the rapid development of ICT technologies and their rapid application to the transport problems makes it possible to develop fairly effective approaches for its solving.

At the same time, the question of development of the traffic organization algorithms themselves remains open. This problem can be solved using game theory, a fairly new but rapidly developing branch of modern mathematics. Unlike optimization theory, which studies the possibilities of constructing an optimal solution for the entire system as a whole, game theory studies ways to optimize individual benefit in competition with other individuals (events) who rationally strive to satisfy their own benefit.

## State-of-the Art

The complexity of analysis of the urban transport flows movement allows us to consider the development and implementation of ITS as a solution for a multi-stage problem, one of the most important stages of solving which is the development of mathematical models of the optimal accident-free movement of vehicles, including the regulation of intersections.

The concept of automatic traffic lights was developed back in 1928, but at that time problems in their application for large cities became apparent (for example, the presence of morning and evening peak hours, which makes it necessary to use the flexible traffic light coordination schemes). Between 1928 and 1930, researchers developed various designs of pressure sensors to detect the presence of vehicles at an intersection. These studies made it possible to create the first models of traffic lights that react to moving traffic (traffic-drive). Such traffic lights operated only on roads where the red light was turned on only if a vehicle appeared from a secondary road (they still exist in the USA).

The first analog controller was installed in 1952 (Denver, USA), which made it possible to combine several disparate intersections into a single controlled network and switch pre-calculated coordination plans depending on the time of day and days of the week. Over the next decade, several hundred similar systems were installed around the world.

Such systems actively used the offset parameter, turning on green not at all intersections at once, but with an offset depending on the distance between intersections and transport parameters ("green wave"). A specially trained engineer calculated coordination schemes, which were then incorporated into the

controllers. The system turned out to be so simple and reliable that it is still actively used in cities that are not burdened with excessive traffic.

The IBM 650B computer was first installed to control traffic lights in 1960 (Toronto, USA). Three years later, more than 20 intersections were under centralized control, and by 1973, the computer was already managing 885 intersections.

It should be noted that IBM continued to work on usage of its computers to control traffic lights: a project began in 1964 with an IBM 1710 computer (downtown San Jose, USA), and in 1965 with an IBM 1800 (a version of the 1130 with an increased number of input/output ports) was installed for the city of Wichita Falls (Texas), which successfully controlled 85 intersections. The computer in San Jose was also subsequently replaced by an IBM 1800. The system turned out to be so successful that this configuration was used in many American cities from Austin and Portland to New York.

An active work on the standardization of traffic light control systems began in 1967. As part of the pilot project, a control system was built for Washington, which included 113 intersections equipped with 512 inductive loop traffic detectors. The computer was able not only to blindly switch coordination plans, but also to receive information about transport queues at intersections.

A critical mass of computer-connected traffic lights had been reached, and the transition from quantity to quality was only a matter of time. Large-scale research has begun in the development of control algorithms.

However, the development of each plan at that time was done on paper and was a rather labor-intensive and creative process, especially for a street network.

In the 70s, the British research bureau TRRL developed and applied the SCOOT (Split, Cycle and Offset Optimization Technique) system on the streets of Glasgow, which made it possible to change the parameters of intersection control cycles in certain frames in accordance with information from traffic detectors that measure the appearance and length of lines on intersections. SCOOT combines the benefits of fixed coordination plans for the network and adaptive control, where traffic lights are controlled by the cycle and duration of green signals. To make a decision on changing the main parameter - the cycle length - a computer with the SCOOT program calculated the so-called degree of saturation of all phases of the traffic light. This indicator was presented as a percentage of the green signal used: the algorithm estimated how many more cars would have time to pass the intersection, filling the gaps between cars (recorded by the sensors). SCOOT's goal was to ensure that even during peak loads, the traffic saturation was no more than 90 percent.

In addition, once during the cycle the program calculated the efficiency coefficient based on the sum of forced stops and car waiting time. Depending on the value of the coefficient, SCOOT made a decision to lengthen or shorten some phase by 4 seconds. Before the start of a new phase, the offset relative to other traffic lights was additionally agreed upon, also within four seconds.

This algorithm is now licensed by more than 100 companies for use in their own systems. The latest generation of SCOOT has a number of features:

- analysis of non-standard situations;
- avoiding the formation of traffic jams;
- smoothing out the consequences of intervention by traffic controllers and temporary shutdowns of traffic flow.

In parallel with SCOOT, simultaneous control systems appeared. The Australian SCATS (Sydney Coordinated Adaptive Traffic System) system has become the main competitor to SCOOT and has also become widespread throughout the world. Based on similar methods for calculating the "saturation" of traffic light phases, an algorithm with a complex hierarchical structure was developed. Intersections in SCATS are grouped into systems and subsystems based on geography (for example, by neighborhood or location on highways). These systems and subsystems are subordinate to the regional computer, and it transmits information to the city traffic control center. Traffic lights can independently change only the length of the cycle, and the schedules of phases and shifts after each cycle are selected (from a standard set) at the regional level (Melekhin 2011).

The difference in management efficiency between adaptive and "intelligent" systems is practically absent now. But with the development and reduction in cost of computers, opportunities arise to increase the levels of survivability and efficiency of management of transport processes and road safety, which are solved by creation of the high-tech automated systems for managing transport and pedestrian flows.

It is impossible to compare directly the effectiveness of all the listed traffic light control systems - to do this, one would have to test each of them in turn in the same city (at the same intersections). Therefore, different algorithms are compared by how much they improved the transport situation (Zelensky 2013).

A new stage in the development of methods and means for regulating intersections is associated with the development of fully adaptive control algorithms, for example RHODES (Real-time Hierarchical Optimizing Distributed Effective System) and OPAC (Optimized Policies for Adaptive Control).

For example, RHODES evaluates the traffic situation at several levels (intersection, road network, common routes) and constructs itself the necessary cycles for traffic lights. The system makes decisions by analyzing not only information from vehicle presence sensors, but also the accumulated history of traffic on controlled streets (links). Based on these data, the system makes a forecast of the development of the traffic situation. A key role in the forecast is played by an algorithm for estimating the probability of a car turning at each specific intersection - this is how the possible load of neighboring intersections is calculated. RHODES takes a statistical distribution of probabilities of turns as a starting point, and then refines this distribution with data obtained over the last five minutes. To refine the forecast, RHODES uses the Bayes formula to calculate the probability of one event (the most popular turn) that is statistically correlated with other events (the turns just completed). This forecast is updated every second for the entire system, and then supplemented with information about expected traffic jams at each intersection. It is worth noting that the system provides a

special mechanism for processing so-called queues of cars - columns that move at approximately the same speed. When such queues appear, traffic light cycles are adjusted to, if possible, allow these vehicles to pass through all intersections without stopping, on the "green wave".

A special case of global traffic forecasts is used by the OPAC system. This algorithm relies on additional information from sensors that are located at a significant distance from the intersection - they transmit data about approaching cars after the decision to change the traffic light cycle is made. As a result, the system's forecast has two horizons: long-term, limited only by computing power, and short-term - for the period of time when the influx of new machines is precisely known. The degree of agreement between the short-term forecast and the actual situation is used to adjust further calculations.

All the systems described above have two characteristic features: they try to improve the situation for all controlled intersections and regulate the operation of traffic lights not directly, but through changing cycles. In 2008, the InSyc system was launched in the United States for the first time, devoid of both of these restrictions. InSync focused on an algorithm in which it is assumed that the optimal local solutions found at individual intersections lead to an optimal global solution - reducing congestion throughout the city. At each intersection, InSync accurately calculated, using cameras and image recognition technology, how long waiting cars waited for the green signal. The traffic lights themselves in the system were controlled not by cycles and schedules, but by automatic models - programs that specified the conditions for changing signals. For example, the algorithm may not turn on "green" at all for a direction in which there are no cars. The system provided this mode only for those cases when it was necessary to skip the line of cars. In this case, the duration of the phases of individual traffic lights was adjusted to form a "green wave". The number of launched "waves" was regulated by the system parameters depending on the time of day and the wishes of the operator.

An interesting approach to traffic control is implemented in the MARLIN-ATSC (Multiagent Reinforcement Learning for Integrated Network of Adaptive Traffic Signal Controllers, Toronto) system. In this development, a centralized system was abandoned - it was replaced by traffic lights - agents (devices that are equipped with artificial intelligence and communicate with each other to select a traffic pattern). The program that is loaded into each traffic light describes the Markov decision-making process, namely, its special case - Q-learning. This principle of machine learning involves communication between an agent (traffic light) and a system (traffic). Each action of a traffic light somehow affects the traffic situation, the change in which can be judged by the information received from the sensors. Having received this information (the so-called reward), the traffic light agent calculates its utility function Q and further relies on the acquired experience.

To coordinate agents among themselves, game theory is used, namely, a stochastic game. During the game, agents go through their decision options (leave or change the traffic light phase) and receive rewards (car idle data) based on general decisions. Each decision of a traffic light agent is tied to a set of indicators

of the current state: which phase is on, how long ago this phase has been on, what kind of traffic jam has accumulated in each direction of the intersection. "Players" must develop behavior patterns that will lead to the best overall result - the so-called Nash equilibrium. The resulting “utility” tables for “state-decision” pairs become the policy that will guide each traffic light in the future. Traffic lights are “trained” on a computer model, and not in real road conditions (Zelensky 2013). The approach is undoubtedly of significant interest, but requires similar research by domestic mathematical schools.

## Methodology

Tactical traffic management for road transport involves monitoring the actual traffic situation in real time (including volumes, speeds, incidents, etc.) and then controlling or influencing flow using this information to reduce congestion, manage incidents, improve efficiency, safety and environmental performance, etc. (Kapsky 2008, Gettman et al. 2008).

On a larger sence, strategic traffic management includes the management of entire networks at a macro level (overall operating policy) as well as the integration or interconnection of different networks. However, urban traffic flows have the following specific properties:

- stochasticity (their characteristics allow prediction only with a certain probability. The traffic flow moves along a transport network, which has certain characteristics that allow a more or less strict description, and is not stationary);
- non-stationary nature of transport flows (fluctuations in their characteristics occur in at least three cycles: around the clock, weekly, seasonal);
- imperfect controllability (even with complete information about traffic flows and the ability to inform drivers about the necessary actions, these requirements are only advisory in nature, therefore achieving the global extremum of any control criterion is very problematic);
- multiple research criteria (average speed, predicted number of accidents, volume of exhaust gases in the atmosphere, etc.). Most of these criteria are interrelated, and it is very difficult to choose just one;
- the difficulty of taking into account even the basic characteristics that determine the quality of traffic flow management. Thus, assessing traffic intensity requires either the use of aerial photography data, or very labor-intensive manual control, etc.

A typical basis for modeling the transportation of goods is a network consisting of links and nodes representing roads and intersections, respectively. In most cases, attempts are made to reduce the complexity of calculations by taking into account only the most important factors when entering an intersection. With these simplifications, processes such as turning left against oncoming traffic can

be modeled, but decisions about the sequence of actions must be made before the vehicle enters the turn.

At the same time, computational forecasts, although absolutely necessary, are not so highly reliable (except in cases where extensive experimental experience was used). The attempts of some specialists, already at the development stage, to predict with high reliability the optimal solution for traffic flows only by calculation, indicate extreme optimism and should be assessed accordingly. Generalization of statistical data and observation results of a single situation or a single object (intersection) are very important for adapting purely mathematical modeling to specific conditions. On this basis, probabilistic estimates related to a specific situation or specific object must be calculated.

The basis of modern automated traffic control systems, which ensure minimization of functionality, is the queue model. In general, the queue dynamics are based on the representation of the regulated direction as a queuing system (Vlasov and Orlov 2014):

$$A(t) = \int_0^t q(t)dt\ ; \tag{1}$$

$$D(t) = \int_0^t S(t)dt\ ; \tag{2}$$

$$Q(t) = Q(0) + A(t) - D(t); \tag{3}$$

$$d = \frac{1}{A(T)} \cdot \int_0^T Q(t)dt, \tag{4}$$

where A(t) is the cumulative number of vehicle's arrivals; D(t) – number of vehicle's handlings during the period [0,t] in the presence of a residual queue of vehicles Q(0); Q(t) – current number of vehicles in the system; d – average delay of vehicles during the period [0,T]; q(t) – intensity of arrival of vehicles; S(t) – intensity of passing vehicles.

A graphical interpretation of the model is shown in Figure 1. It should be noted that the functions A(t), D(t), Q(t) are generally probabilistic in nature. However, in the case of ITS they can be considered as deterministic functions.

Most modern automated traffic control systems have tools that implement the following control strategies:

- rationing of entry into the transport congestion zone;
- providing priority in selected areas;
- preventing directions from being blocked.

It should be noted that when developing strategies in transport systems, two approaches are considered, which consist in analyzing and resolving the following situations:

- building a strategy to avoid traffic congestion;

- development of a strategy that allows, in the event of a congestion, to eliminate it in a minimum period of time.

Moreover, in conditions of transport congestion, as a rule, various expert systems are used, the tasks of which are to identify the current situation and apply the appropriate control strategy (Vlasov and Orlov 2014, Klimovich 2018). At the same time, an approach based on building a network of "intelligent" traffic lights exchanging information is of significant interest.

Let us consider the solution to the problem in a general formulation. A typical traffic pattern at a traffic intersection is shown in Figure 2. It should be emphasized that modern diagnostic tools and the use or broadcast of relevant V2I or V2V data make it possible to quite accurately determine all the data necessary for the analysis of traffic flows. Thus, in this case, the goal of managing traffic flows at an intersection can be formulated as follows: the optimal time of the "green" traffic light signal for each traffic lane must be determined so that the average delay time in directions, described by formula (4), is minimal.

**Figure 1.** *Graphical Interpretation of Transport Queue Formation*

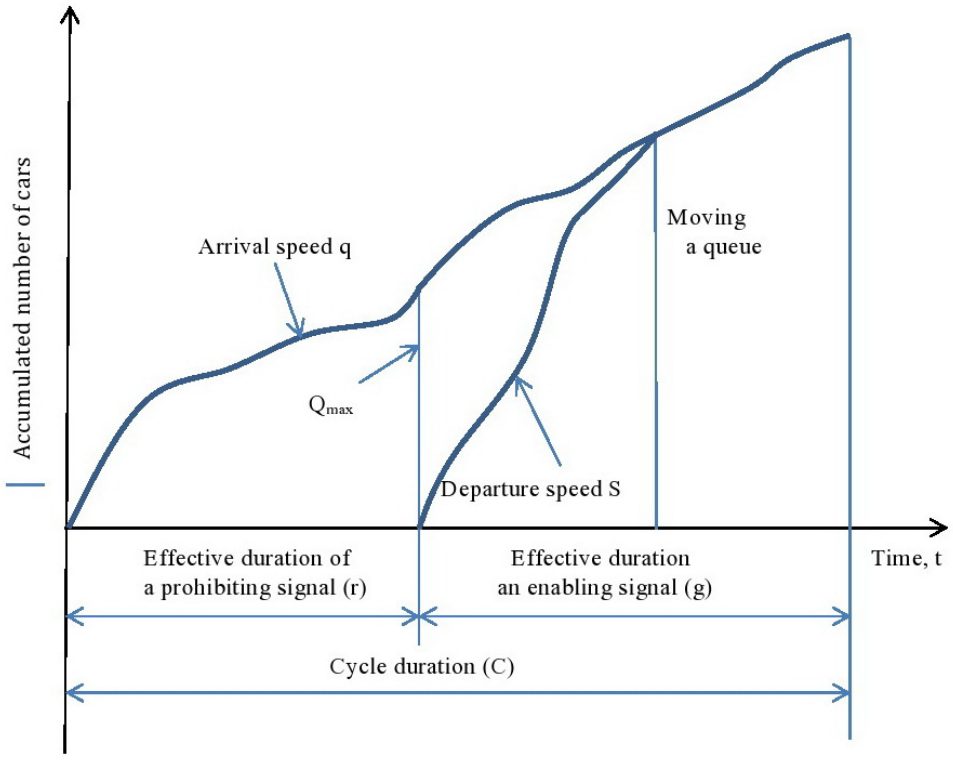


The solution of this problem can be carried out in accordance with game theory - a fairly new, but rapidly developing part of modern mathematics. Unlike optimization theory, which studies the possibilities of constructing an optimal solution for the entire system as a whole, game theory studies ways to optimize individual benefit in competition with other individuals (events) who rationally strive to satisfy their own benefit. With this consideration, the traffic delay is

determined by the delays in the directions $R_{11}$, $R_{12}$, $R_{21}$, $R_{22}$, and its optimal value can be considered a win in a non-zero-sum game.

**Figure 2.** *The Scheme of Traffic at the Intersection*

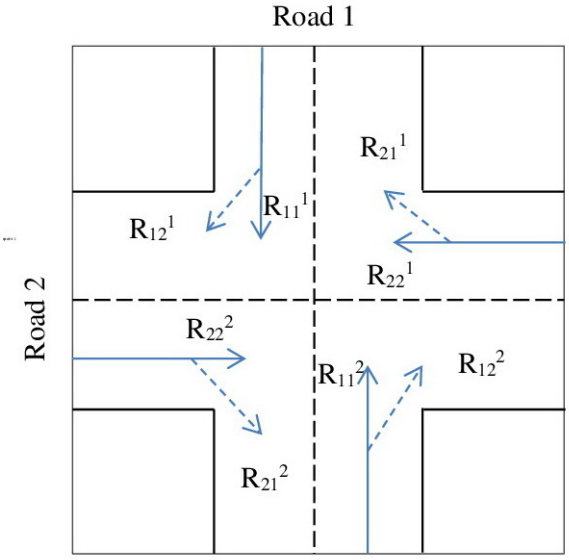


The assessment of the gain (the amount of traffic flow delay) can be carried out from the point of view of the minimax theory (the lower bound of the estimate is the minimum but guaranteed gain), as well as from the point of view of constructing an equilibrium solution (a strategy according to which any attempt by any player to change his strategy when his partner insisting on the original choice will not increase the winnings of the player violating the strategy).

Let us develop a payment matrix for this formulation of the problem:

$$\begin{array}{c|cc} & \multicolumn{2}{c}{Road\ 2\,(player\ 2)} \\ Road\ 1\ (player\ 1) & R_{11} & R_{12} \\ R_{21} & (d_{11}^1, d_{11}^2) & (d_{12}^1, d_{12}^2) \\ R_{22} & (d_{21}^1, d_{21}^2) & (d_{22}^1, d_{22}^2) \end{array}, \quad (5)$$

where $d_{ij}$ is the total traffic delay, calculated using formulas (1 - 4) for the corresponding road lanes.

The analysis of such a payment matrix is carried out using known methods. Player preferences are usually indicated by arrows (the direction corresponds from smaller to larger winnings). The equilibrium point is defined as the point indicated by the vertical arrows (the first player's preference for the first strategy due to the higher payoff associated with it) and the horizontal arrow (the second player's preference). Obviously, in accordance with this formulation, the equilibrium point (A, B) can be found using the formula:

$$A = \max_i \{d^{(j)}_{(i.j)}\},$$
$$B = \min_j \{d^{(i)}_{(i,j)}\}, \quad i, j = \overline{1,2}. \qquad (6)$$

The guaranteed level and maximin strategy can be determined without knowing the actions of the other player. However, based on this method of constructing the payoff matrix, it can be obtained that the results of the maximin theory are identical to the equilibrium point. The question remains open in what sense the winning and the corresponding strategy are the best. It is believed that the player guarantees himself the maximum (and possibly the largest) winnings using an equilibrium strategy (Saati 1977). After determining the equilibrium strategy (and, therefore, up to the maximum guaranteed gain, for example, the delay time of vehicles moving in the corresponding directions), it is possible to draw a conclusion about the most significant traffic delays for the current transport situation.

Let's consider an intersection (Figure 2), at which the average delay of vehicle movement along the considered lanes at the intersection is indicated in Table 1.

**Table 5.** *Distribution of Average Traffic Delays at an Intersection by Lane*

| The road lane | Direction of movement | An average traffic delay, min |
|---|---|---|
| $d^1_{11}$ | straight | 1.0 |
| $d^2_{11}$ | straight | 2.0 |
| $d^1_{12}$ | right turn | 2.0 |
| $d^2_{12}$ | right turn | 1.0 |
| $d^1_{22}$ | straight | 3.0 |
| $d^2_{22}$ | straight | 0.0 |
| $d^1_{21}$ | right turn | 2.0 |
| $d^2_{21}$ | right turn | 1.0 |

It should be noted that modern means of information and communication technologies make it possible to determine the number of cars and the direction of their movement quite accurately). The payoff matrix for this case of a traffic situation at the intersection of two roads $R_1$ and $R_2$ has the form:

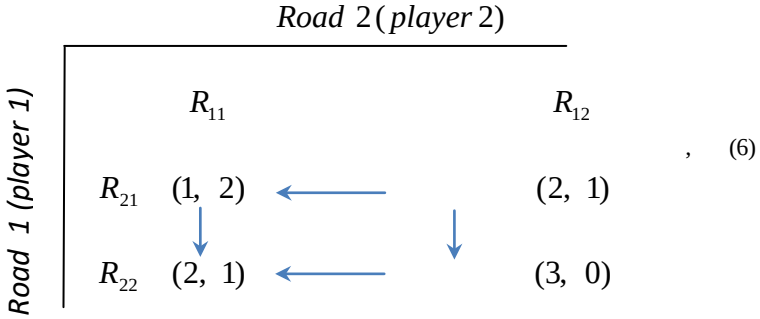


, (6)

It is obviously, the solution can be based on pure strategies. The matrix under consideration has a saddle point - (2, 1). In this case, the gain (average delay of cars) is equal to:

- 2.0 minutes for the $R_1$ road;
- 1.0 minutes respectively for the $R_2$ road.

From these data, using formula (4), it is possible to calculate the duration of the period T in each direction and, accordingly, determine the operating order of "intelligent" traffic lights.

Another case of analyzing the distribution of average traffic delays at an intersection is also possible, in which the distribution of the number of cars is indicated in Table 2.

**Table 2.** *Distribution of Average Traffic Delays at an Intersection by Lane*

| The road lane | Direction of movement | An average traffic delay, min |
|---|---|---|
| $d_{11}^1$ | straight | 5.0 |
| $d_{11}^2$ | straight | 2.0 |
| $d_{12}^1$ | right turn | 3.0 |
| $d_{12}^2$ | right turn | 3.0 |
| $d_{22}^1$ | straight | 5.0 |
| $d_{22}^2$ | straight | 1.0 |
| $d_{21}^1$ | right turn | 2.0 |
| $d_{21}^2$ | right turn | 3.0 |

The payoff matrix for this case of a traffic situation at the intersection of two roads $R_1$ and $R_2$ has the form (7).

Obviously, there is no solution in pure strategies for this matrix. Let us find this solution in mixed strategies.

To ensure that the average delay time of cars is minimal (or close enough to this value) on road $R_1$ (player 1), regardless of the delay of cars on road $R_2$ (player 2), we will focus on the average delay of cars on road $R_1$, etc. So let us calculate the mixed strategies defined for $R_2$.

In accordance with the terminology of game theory, if player 2 chooses the first column of the payoff matrix with probability q, and the second column with probability 1-q, then the mathematical expectation for both rows of player 1's winning matrix must be equal, that is:

$$5 \cdot q + 2 \cdot (1 - q) = 3 \cdot q + 5 \cdot (1 - q)$$

Therefore, q= 3/5, 1- q = 2/5.

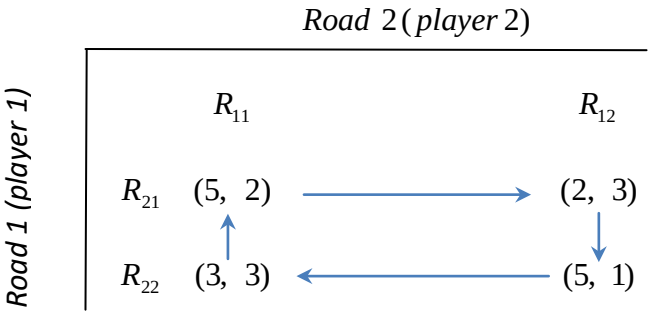


, (7)

Thus, player 1 must choose the first column of the payoff matrix with probability 3/5, and the second column with probability 2/5. In this case, the expected winnings of player 1 will be equal to 19/5.

As is easy to see, this value of expected payoff will remain the same when player 1 uses any mixed strategy (p, 1-p), since

$$5 \cdot q \cdot 3/5 + 2 \cdot q \cdot 2/5 + 3 \cdot (1-q) \cdot 3/5 + 5 \cdot (1-q) \cdot 2/5 = 19/5.$$

Just as player 1, wanting to ensure that expected payoff of the player 2 does not depend on his choice of a mixed strategy, using payoff matrix of the player 2, it can be obtained:

$$2 \cdot p + 3 \cdot (1-p) = 3 \cdot p + 1 \cdot (1-p)$$

Therefore, p=2/3, 1-p = 1/3.

Then the mixed strategy looks like:

$$(s_1, s_2) = (2/3 \cdot A_1 + 1/3 \cdot A_2) + (3/5 \cdot B_1 + 2/5 \cdot B_2),$$

and the equilibrium payoff will be (A, B) = (19/5, 7/3).

In this case, the equilibrium gain (average delay of cars) is equal to:

- 3.8 minutes for the $R_1$ road;
- 2.3 minutes respectively for the $R_2$ road.

From these data, using formula (4), it is possible to calculate the duration of the period T in each direction and, accordingly, determine the operating order of "intelligent" traffic lights.

## Results and Discussion

Despite a number of problems that arise during the development and implementation of ITS, the future of the transport industry is undoubtedly

associated with digitalization and the implementation of solutions one way or another related to artificial intelligence. However, the solution to this problem is connected with the implementation of a complex of complex, diverse works, in which an important place is occupied, in particular, by the development of mathematical algorithms for traffic movement.

The article presents an algorithm based on the application of game theory, the implementation of which will allow optimizing traffic at transport intersections by constructing a method of analysis for the entire system as a whole. The solution of the problem in pure and mixed strategies is considered for specific examples.

Usage of this algorithm can become an integral part of the development of ITS in terms of “intelligent” traffic control at traffic intersections.

## Conclusions

The development of new technologies to optimize the driving process is an urgent problem. One of the most promising ways to improve urban logistics is the use of intelligent transport systems. However, in busy traffic conditions, it is not enough to evaluate only the delay and the number of vehicles in the queue. To fully describe the process of formation of traffic congestion in networks with traffic light regulation, it is necessary to use models that describe the spatiotemporal heterogeneity of traffic flow.

Therefore, development and implementation of new algorithms, including those based on game theory, which will improve real-time traffic control and control capacity at intersections will significantly improve the environmental friendliness of urban transport and improve its safety. Using the proposed model, based on the application of game theory, can significantly reduce vehicle delays.

## References

Gettman D, Pu L, Sayed N (2008) *Surrogate safety assessment model and validation: final report*. Publication FHWA-HRT-08-051. FHWA, U.S. Department of Transportation.

Hiertz GR (2010) The IEEE 802.11 Universe. *IEEE Communications Magazine* 48(1): 62–70.

Kapsky DV (2008) *Forecasting accidents in road traffic*. Minsk: BNTU.

Klimovich AN, Shut VN (2018) Algorithm for controlling an intersection based on V2I interaction. *System Analysis and Applied Informatics* 4: 21–27.

Melekhin A (2011) *ATCS: Evolution of "intelligent" traffic lights*. HABR.

Saati TL (197) *Mathematical models of conflict situations.* M.: Soviet radio.

Vlasov AA, Orlov NA (2014) *Managing heavy traffic flows in c*ities. Penza: PGUAS.

Zelensky M (2013) *What needed to be resolved: how mathematics fights traffic congestion*. LENTA.RU.

*Athens Journal of Sciences- Volume 11, Issue 1, March 2024 – Pages 55-74*

# An Analysis of Stream Flow and Flood Frequency: A Case Study from Downstream of Kelani River Basin, Sri Lanka

*By Kumudika K.E. Perera*[*]

*River floods in Sri Lanka are mainly associated with extreme rainfall events. The Kelani and Kalu rivers are recorded the highest flood frequencies and the accompanying flood damages among the river basins in wet zone (UNDP, 2011). Therefore, the specific objective of the study is to estimate the temporal probability of occurrence of flood events in downstream of Kelani river basin. Secondary data were used for the study. Daily discharges data were obtained from Hanwella gauging station for the period of 1990 to 2019 from the Department of Irrigation, Sri Lanka. Trend analysis, normal distribution and flood frequency analysis have been used. The results of the study revealed that there was a bi-modal pattern of discharges that occurred in June and October. The results also indicated that ten return periods were covered the total period of 30 years, and there was a 97 per cent probability of flood occurrence almost annually and 64 per cent probability of occurring once every two years. This study, therefore, was recommended to design flood control structures for mitigating flood risk; and to determine the economic value of flood control projects and the effect of encroachments on flood plain.*

**Keywords:** *floods, frequency, downstream, return period, probability*

## Introduction

Global climate change has led to an increase in the magnitude, frequency, and intensity of natural disasters over the years (Perera 2017). By analyzing the historical and recent data, many scientific studies have revealed that, floods are the most catastrophic and frequently occurring natural disaster together with damaging in terms of cumulative and annual expected losses over the world. According to the United Nations International Strategy for Disaster Reduction (2017), over the last 20 years from 1995 to 2015, floods were responsible for 47 per cent of all weather-related disasters, affecting 2.3 billion people (56 per cent), the majority of whom (95 per cent) live in Asia. Further, the number of floods per year has risen to an average of 171 in the period from 2005 to 2014, up from an annual average of 127 in the previous decade. Because of flood is a component of hydrological cycle of drainage basin (Baishya 2013) and flooding therefore cannot be stopped. However, their impacts may be mitigated and managed to some extent.

Therefore, due to the global climate change, flood risk is a significant issue in many countries all over the world. Sri Lanka is one of such countries which have seasonal flooding problem since seasonal flooding is more frequent and common occurrence in Sri Lanka than the other natural disasters (Jegarasasingam 2017).

[*]Graduate Student, Institute of Human Resource Advancement, University of Colombo, Sri Lanka.

Especially, variability of both annual and seasonal rainfall in Sri Lanka has increased during recent decades due to climate change. Jayawardena et al. (2017) have noted that changes in annual as well as Southwest monsoon seasonal rainfall compare to the baseline climatology period from 1975 to 2005, clearly indicate that positive rainfall anomaly in the wet zone will be risen with the time under high as well moderate emission scenarios.

Accordingly, when considering to Sri Lanka, the country has experienced several notable flood events in more recent years. The Global Climate Risk Index Report 2019, which launched at the Climate Summit in Katowice (COP 24), ranked Sri Lanka as the second among the most affected countries by extreme weather events. The ranking was regarding the heavy landslides and floods after strong monsoon rains in the Southwestern region of the country in 2017. Consequently, the Kelani river basin experienced a total of 350 mm of rainfall across three days from 15$^{th}$ to 17$^{th}$ May in 2016 after the devastating flood in 1989. 23 Divisional Secretariats (DS) divisions (out of 37) in the Kelani river basin were affected by the 2016 Flood. Out of them, 15 DS divisions were affected significantly.

According to the Ministry of Disaster Management in Sri Lanka (2016), the Colombo district has affected 228,871 members of 54,248 families in the 10 DS divisions consisting of Colombo, Homagama, Kaduwela, Kesbawa, Kolonnawa, Kotte, Maharagama, Padukka, Seethawaka and Thimbirigasyaya, while the Gampaha district has affected 74,003 members of 17,485 families in the 13 DS divisions consists of Attanagalla, Biyagama, Divulapitiya, Dompe, Gampaha, Ja-ela, Katana, Kelaniya, Mahara, Meegamuwa, Meerigama, Minuwangoda and Wattala. This flood was characterized by low peaks and longer duration of inundation owing to the rainfall distribution pattern over the catchment (Hettiarachchi 2020). By far the worst affected division countrywide is Kolonnawa where 155,062 people were affected, which is 81 per cent of the total population in this division. In this context, flood hazard is the most significant issue in downstream of the Kelani river basin than the other extreme events.

Especially, downstream of the Kelani river basin has consisted of nine sub-drainage basins namely, Lower Kelani Ganga, Pallewela Oya/ Maha Ela, Lower Middle Kelani Ganga, Kolonnawa Ela, Biyagama, Pagoda Oya, Upper Middle Kelani Ganga, Wak Oya/Kalatuwawa, and Pusweli Oya. Downstream of the Kelani river basin overlaps with four districts (Colombo, Gampaha, Kalutara, and Ratnapura) as well. Therefore, a large area is inundated almost annually due to the floods in the Kelani river.

Further, according to the Department of Irrigation in Sri Lanka (2020), the main causes for recent flooding in the Kelani river are high-intensity rainfall occurred within a short duration, the inadequacy of the drainage system to cater for a higher return period rainfall, flow hindrances in secondary canal system causing localized flooding, unauthorized constructions encroaching water bodies, the inadequacy of outfall capacity of the drainage network, reduction of retention areas, and dumping of solid waste into canals result in the reduction of capacity. In addition to that, other indirect causes of flooding in the Kelani river basin are lack

of investment for drainage projects, unplanned town development, lack of co-ordination among Agencies, and lack of public awareness.

The Kelani river basin suffers from floods mostly during South-west monsoon (SWM) and it causes serious damages to human lives and their properties in the lowland areas of the flood plain almost annually. However, the catchment receives considerable amounts of rainfall during North-east monsoon (NEM), and inter-monsoonal periods too (Hettiarachchi 2020). Due to the heavy rainfall and the steep terrain of the upper catchment, lower basin of the Kelani River is subjected to heavy floods. Especially, the Floodplain is formed below Glencourse gauge which is about 53 kilometers upstream of the sea outfall. Below Hanwella (about 35 kilometers from the sea), the flood plain becomes wider following the flat landscape (Hettiarachchi 2020).

Furthermore, due to the relatively small island setting, the demand for land in the growing urban areas has led to the expansion of cities to land prone to flooding, and which are often deemed unsuitable for habitation (Dissanayake et al. 2018). The outskirts of the metropolitan region of Colombo are pushing into wetlands along the Kelani river basin, which results in environmental degradation and increased exposure of the local population. Many of these settlements are built up on floodplains, which means that the poorest demographics are most vulnerable to flooding events and habitually end up being displaced (United Nations Office for Disaster Risk Reduction 2019).

As has mentioned before, the downstream of the Kelani river basin is a highly populated zone and high distribution of agricultural lands in the river basin. Similarly, due to the barriers of drainage systems in the area because of the construction and extension of utility services, and due to the formation of some areas as marshy lands, there had been small-scale floods. Together with, the marshy lands and water retaining area affected by the canal network in downstream of the Kelani river basin form the land suitable for Paddy cultivation, but still, crop damages occur due to severe flooding in this region (UDA 2019). Floodwaters transport sediments and nutrients to enrich the soil, which is deposited on flood plains. Among the agricultural land uses, paddy lands are flooded purposely to take advantage of this natural fertilization process. However, the exact loss of paddy production will depend upon several factors including crop variety, the growth stage of the plant, level of inundation or flood depth, and length of flooding period of duration.

Moreover, People tend to gather close to rivers or concentrate in the coastal areas because water is a resource before being a threat, and therefore a high level of risk, in flood-prone areas, a tendency will likely increase in future. Owing to the adverse nature of flooding in Sri Lanka, it is needed to do many researches and identify the best practices regarding to the flood management. In this regard, stream flow and flood frequency analyzes are primary steps in the flood control process because it is essential for the identification and prioritization of the top priority areas, selecting the best practices and best designs to flood reduction and land use planning. Therefore, this research will try to the analysis of flood occurrences. This will further help to design the appropriate land use planning and

engineering measures in flood-prone areas and managing the annual flood menace in downstream of the Kelani river basin.

Accordingly, the main objective of the study is to analyze the stream flow and flood frequency in downstream of the Kelani river basin. The specific objective of this study is to estimate the temporal probability of occurrence of flood events between 1990 and 2019.

## Literature Review

A flood is a natural hazard that can be categorized as hydro-meteorological hazard. A flood can be simply defined as water overflowing onto usually dry land. However, different definitions can be adopted to describe flood events. USGS (2020) defines a flood as "any relatively high stream flow overtopping the natural or artificial banks in any reach of a stream". Furthermore, hydrologists define floods as a sudden peak in the water level due to the sudden increase in water discharge. Therefore, floods occur because of the rapid accumulation and release of runoff waters from upstream to downstream, which is caused by extremely heavy rainfall.

### *Characteristics of Floods*

According to Van Westen et al. (2011), flood can be characterized by the triggering factors, spatial occurrence, duration of the event, time of onset, frequency, magnitude and secondary events. These characteristics can help in categorization of different types and levels of flood as well as it enable to compare different hazards with each other. Therefore, floods can be triggered by different natural and anthropogenic phenomena. Sometimes it is prolonged rainfall that causes floods, sometime torrential rains or storms cause flooding situation.

Spatial occurrence refers to the area and the extent of the area affected by the flood. Floods do not occur randomly. They occur in areas that are in geographical proximity to water bodies, where prolonged rainfall occurs or in areas with poor drainage system. These characteristics enable to categorize the flooding events. The extent of the area covered by the flood can be small for example in the case of flash floods; it affects only a village, town, or a city. While riverine floods can affect many a city on its way (Van Westen et al. 2011).

Duration of the event means the time span between the start and end of the flooding or the event that caused the flood. Usually this is difficult to be defined for floods as the recede very slowly and does not vanish completely, rather the flood water moves from one area to another. When attention to the time of onset of the flood, it is the time span between the start of the event causing the flooding and the time when the flood has actually occurred, for instance, the delay between the rainfall and the peak discharge.

Figure 1 represents the temporal relation between discharge rate and rainfall in a monsoonal area. In the figure, two flood events are recorded: the first at the $11^{th}$ day, and the second, smaller than the previous, at the $29^{th}$ day; they are caused

mainly by the rain fallen in the 8th day, and in the 21st day. The figure also represents the area with blue stripes and the two arrows show the time lapse between the precursor (rainfall) and the hazard pick (flood max discharge) (Van Westen et al. 2011).

**Figure 1.** ***Discharge - Rainfall Relationship***

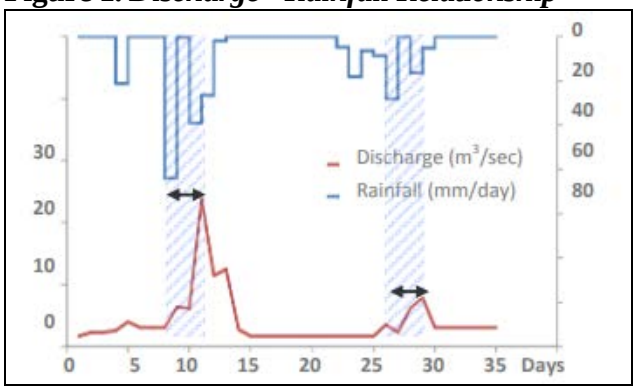


Frequency of flood events mean how often the flooding occur in a given time period, for example, a year. Flood recurrence intervals can range from multiple times a year to once in 10 years or even 30 years. It allows scientists/ researchers to understand when a flood of certain magnitude and intensity will occur in a given area. Magnitude refers to the energy released during the hazardous event (Van Westen et al. 2011).

Seasonality refers to the season that has the most probability for flood. In South Asia including Sri Lanka, the probability of floods is highest in Monsoon period (July - August) as compared to the rest of the year. This is due to the seasonal winds (monsoon) that blow over South Asia in this period. By knowing the season for the flood hazard, it can be taken steps to prevent, mitigate or in the worst case prepare for the hazard (Van Westen et al. 2011).

Intensity of floods is the damage caused by it. It can be characterized by depth of inundation, volume of inundation, velocity of flow and rate of rise of water. The more the depth of water, more will be its volume, velocity, and its damaging capacity. A high rate of rise for water also means less preparation time for people in the area (Van Westen et al. 2011).

*Types of Floods*

Floods can be categorized in different ways based on several criteria. According to their duration, flood can be divided into different categories as Slow-onset floods, Rapid-onset floods, and Flash floods. Also, floods can be categorized according to the water source (origin), geography of receiving area, cause, and the speed of onset. The water source of floods can originate from the ocean (coastal floods), rivers (fluvial floods), from underground (groundwater floods) and from rain (pluvial floods) (EC 2020, Klijn 2009).

Floods in Sri Lanka can be classified in several different ways. One of the more common and useful ways of classifying floods is based on the source and the

nature of flooding. Accordingly, the types of floods are riverine floods, flash floods, localized floods, floods caused by reservoir operation and floods caused by reservoir breaching (Disaster Management Centre 2012).

*Triggering and Causative Factors of Flooding*

Floods can be triggered by different natural and anthropogenic phenomena. Sometimes, it is prolonged rainfall that causes floods, and sometimes torrential rains or storms cause flooding situations. However, floods are not always triggered by heavy rainfall. They can result from other phenomena, particularly in coastal areas where inundation can be caused by a cyclone, a tsunami, or a tidal surge due to attractive forces of the sun and the moon. Dam failure also results in flooding of the downstream area, even in dry weather conditions. Further, in the dry season, high average temperature can result in increased melting of the snow, hence high discharge downstream in some countries especially in India. Similarly, lack of permeable surface and high groundwater table in a region can also trigger a flood. On the other hand, as an endogenic factor, floods can be caused by earthquakes (Van Westen et al. 2011).

When focused on causative factors, floods mainly occur due to unplanned rapid growth and development of urban areas interfering with floodplains (Balabanova and Vassilev 2010). The additional causes of floods are deforestation, climate change, change in weather patterns, improper waste management, changes in land use, bad farming practices, poor dam construction, as well as the characteristics of the catchment area, drainage network, and the river channels. The triggering and causative factors of flooding are shown in Table 1.

**Table 1.** *Factors Contributing to Flooding*

| Meteorological Factors | Hydrological Factors | Human factors aggravating natural flood hazards |
|---|---|---|
| • Rainfall<br>• Cyclonic storms<br>• Small-scale storms<br>• Temperature<br>• Snowfall and snowmelt | • Soil moisture level<br>• Groundwater level prior to storm<br>• Natural surface infiltration rate<br>• Presence of impervious cover<br>• Channel cross-sectional shape and roughness<br>• Presence or absence of over bank flow, channel network<br>• Synchronization of run-offs from various parts of watershed<br>• High tide impeding drainage | • Land use changes (e.g., surface sealing due to urbanization, deforestation) increase runoff and may be sedimentation<br>• Occupation of the flood plain obstructing flows<br>• Inefficiency or non-maintenance of infrastructure<br>• Too efficient drainage of upstream areas increases flood peaks<br>• Climate change affects magnitude and frequency of precipitation and floods<br>• Urban microclimate may enforce precipitation events |

*Source:* Van Westen et al. 2011.

*Flood Patterns in Sri Lanka*

Floods are the most common and hazardous natural event than the other natural disasters in Sri Lanka. Especially, there is a significant spatial and temporal pattern of river floods in Sri Lanka. When considering the annual flood pattern, it can characterize by two distinct monsoon seasons, specifically the SWM (from May to September) and NEM (from December to February). Therefore, the country is subjected to floods twice a year. The rainfall distribution pattern during SWM and NEM in Sri Lanka is illustrated in Figure 2. According to Figure 2, the SWM brings heavy rains to the western and southern slopes of the central highlands while the NEM brings rains to the eastern side of the central hills and lowlands. Therefore, major riverine floods are mainly associated with extreme rainfall received during the above two monsoon seasons.

**Figure 2.** *Spatial Pattern of Rainfall in SWM and NEM Seasons in Sri Lanka*

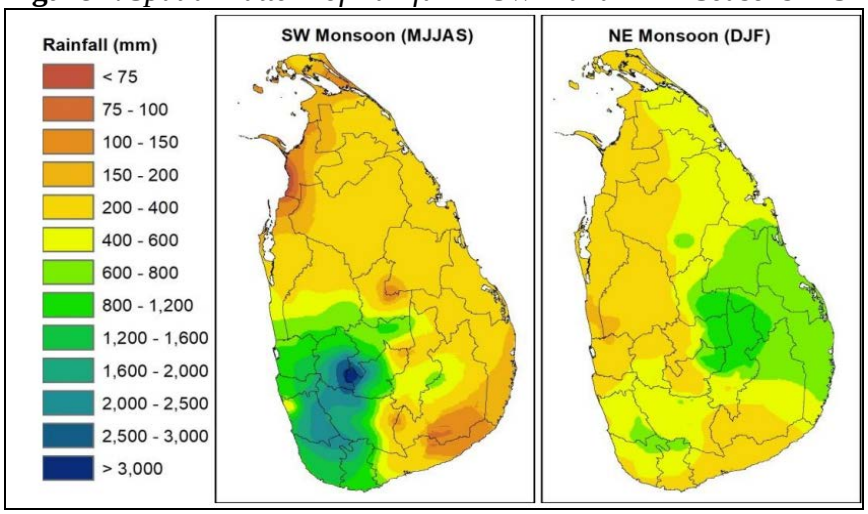


In addition to these monsoon seasons, the country receives torrential rainfall because of the development of low-pressure systems or tropical cyclones frequently form in the Bay of Bengal. Accordingly, most of the cyclonic floods occur from October to December (Basnayake et al. 2019). As well, historical records show that most cyclones hit the east, north, and north-central areas of the island (Yoshitani et al. 2007). The Vavuniya district shows a higher flood probability due to cyclonic storms. Even though the annual rainfall is lower than the Western highlands, Vavuniya and Mullaitivu in the north have recorded the highest rainfall intensities in the island (Zubair et al. 2020).

*Flood River Basins in Sri Lanka*

Among the major river basins, the Kelani, Gin, Kalu, Nilwala, and Mahaweli rivers are more vulnerable to the occurrence of floods. Therefore, they can be called as main flood-prone basins in Sri Lanka. Especially, according to the UN-Water (2006), 36 major river basins out of 103 natural river basins have been

classified into three main groups as south-west monsoonal; north-east monsoonal; and both monsoonal river basins.

Accordingly, the Kalu, Kelani, Gin, Nilwala, and Bentota rivers; the Attanagalu Oya, and the Maha Oya in the wet zone are included in group one viz. south-west monsoonal river basins. These rivers are more subjected to floods triggered by the SWM that arrives in late May, thus the districts of Kalutara, Kegalle, Gampaha, Ratnapura, Colombo, and Gall are inundated (Disaster Management Centre 1999). However, the Kelani and Kalu rivers are recorded the highest flood frequencies and the accompanying flood damages among the river basins in the wet zone (United Nations Development Programme 2011). The slight gradients encountered in lower parts of the river mainly cause the floods in the Kelani river basin due to the extremely heavy and prolonged rainfall in the upper catchment areas.

Further, according to the UN-Water (2006), 26 river basins, including the Mahaweli river, Maduru Oya, Kirindi Oya, Maha Oya, Mee Oya, Deduru Oya, Malwathu Oya, and Mundeni Aru are fallen into group two viz. northeast monsoonal river basins. These river basins are in the dry zone and covered a significant spatial distribution of the country. Therefore, a large area of the country is inundated during the NEM due to the heavy rains.

The Mahaweli river in the dry zone and the Walawe river basin, which spreads across the semi-arid zone of the southern part of the country are included in the third group viz. receiving rainfall from both monsoon seasons. Accordingly, the Mahaweli and Walawe rivers can call as bi-monsoonal rivers. In addition to that, the Deduru Oya also falls into the third group. However, this river is not strictly bi-monsoonal.

*Effects of Flooding*

Floods are one of the most frequent occurring natural disasters that directly and indirectly has sever effects on human and the environment (Hewitt 2013). The direct damages are those who cause harm by contact of flood water with property, humans, or other objects. Indirect damages are those who occur outside the flood event itself (World Meteorological Organization 2008). The most important parameters influencing flood impact are water depth, duration of flooding, flow velocity, sediment concentration, sediment size, wave or wind action, pollution load of flood water and rate of water rise during flood onset (Genovese 2006). The losses due the floods are shown in Table 2.

**Table 2.** *Categorization of Flood Losses*

| | **Tangible Direct Losses** | **Tangible Indirect Losses** | **Intangible Human and Other Losses** |
|---|---|---|---|
| **Primary** | Damage to:<br>• Buildings (e.g., houses)<br>• Contents of buildings<br>• Infrastructure (e.g., roads, bridges)<br>• Crops and animals | Loss of, or disruption, to:<br>• Agricultural production<br>• Industrial production<br>• Communications (e.g., road, rail, and telecommunications)<br>• Health care and education services<br>• Utility supplies (e.g., electricity) | • Loss of life<br>• Physical injury<br>• Loss of heritage or archaeological site |
| **Secondary** | • Flood causes fire and fire damage<br>• Salt in seawater contaminates land and reduces crop yields<br>• Flood cuts electricity supply, damaging susceptible machines and computer runs | • Lost value added in industry<br>• Increased traffic congestion and costs<br>• Disruption of flow of employees to work causing "knock-on" effects<br>• Contamination of water supplies<br>• Food and other shortages<br>• Increased costs of emergency services<br>• Loss of income<br>• Increased household costs | • Increased stress<br>• Physical and psychological trauma<br>• Increase in flood-related suicides<br>• Increase in water-borne diseases<br>• Increase in ill health<br>• Increase in post-flood visits to doctors<br>• Hastened and/or increased mortality |
| **Tertiary** | • Enhanced rate of property deterioration and decay<br>• Long-term rot and damp<br>• Structures are weakened, making them more damage prone in subsequent floods | • Some businesses are bankrupt<br>• Loss of exports<br>• Reduced national gross domestic product | • Homelessness<br>• Loss of livelihoods<br>• Total loss of possessions (i.e., uninsured)<br>• Blighted families<br>• Lost communities where communities are broken up |

*Source:* World Meteorological Organization 2008.

Floods can also bring positive effects of many benefits such as recharging ground water, making soil more fertile and increasing nutrients in some soils. Especially, flood waters provide much needed water resources in arid and semi-arid regions where precipitation can be very unevenly distributed throughout the year. Freshwater floods particularly play an important role in maintaining ecosystems in river corridors and are a key factor in maintaining floodplain biodiversity. Also, flooding can spread nutrients to lakes and rivers, which can lead to increased biomass and improved fisheries for a few years. For some fish species, an inundated floodplain may form a highly suitable location for spawning with few predators and enhanced levels of nutrients or food. Fish such as the

weather fish make use of floods in order to reach new habitats. Bird populations may also profit from the boost in food production caused by flooding.

*Recent Trends in Floods of Sri Lanka*

The nature of catastrophic floods has also changed in recent years in the world with an increase in the frequency of flash floods, acute riverine, and coastal flooding. Besides, urbanization has significantly increased flood runoffs, while recurrent flooding of agricultural land, particularly in Asia, has taken a heavy toll in terms of lost production, food shortages, and rural under-nutrition (United Nations International Strategy for Disaster Reduction 2017). Therefore, the occurrence of flood events shows an increasing trend in most regions of Sri Lanka. According to the study of national climate change adaptation strategy for Sri Lanka - 2011 to 2016 undertaken by the Environmental Ministry of Sri Lanka, it has been reported that increased the intensity of rainfall in the wet zone due to climate change is expected to increase the propensity for flooding in flood-prone rivers (Perera 2017).

Further, the total number of flood events in Sri Lanka is recorded high. According to the historical data, flood events have increased over the years with 25 large floods that occurred between 2000 and 2013 due to the intensity and frequency of extreme weather events. Intense rainfall above 300 mm within 24 hours caused to occur flash floods in 2010, 2011, and 2012 due to the climate change impacts.

Moreover, with an increase in the number of flood events, the associated flood damages such as the number of building damages, crop damages, and infrastructure damages have been also increased. Further to this, another flood impacts such as the number of injuries and affected people have also sharply increased as obvious from the past few years. However, there is a significant decline in loss of lives due to flooding since 2003 (Consortium of Humanitarian Agencies 2016).

The number of districts affected by floods has also increased. According to the Consortium of Humanitarian Agencies (2016), the most vulnerable districts which were affected by floods during the last 40 years from 1974 to 2015 are Batticaloa, Ampara, Colombo, Gampaha, Kalutara, and Ratnapura districts respectively. In addition to that, the Hambantota district can be identified as a new vulnerable district in Sri Lanka affected by floods from 2000 to 2013. Accordingly, Hambantota, Tissamaharama, and Ambalantota divisions are prone to flood in this district.

## Theoretical Review

*Trend Analysis*

A common feature of time series data is a trend. Using regression, we can model and forecast the trend in time series data. Accordingly, in this study, linear

regression analysis was used to analyze the stream flow pattern in the downstream of the Kelani river basin. A regression based trend analysis was conducted using linear trend model by using the following equation.

$$Y = mx + c \qquad \text{Equation (1)}$$

Where *m* represents the rate of changes and *c* represents the *y* intercept of the line. The R-squared ($R^2$) value ranging from '0' to '1' or the 'corrected R squared' ($R^2$) which is adjusted for degrees of freedom indicates the explanatory power (goodness of fit) of the model.

*Flood Frequency Analysis*

Flood frequency analysis is one of the significant studies of river hydrology (Yadav 2002). It is based upon the historical records and provides an estimate of exceedance probability or recurrence interval of the flood of a particular magnitude (Gilard 1996). This is analyzed based on the maximum rainfalls, maximum discharges, or water levels, which is the largest instantaneous peak flow occurring at any time during the year by Gumbel's method, Log-Normal and Log Pearson III Type method. The estimation of the frequencies of the flood is important to understand the previous records of flood events to evaluate future possibilities of such occurrences.

In this study, the flood frequency analysis was done by using Gumbel Extreme Value Distribution. Gumbel's extreme value distribution which is one of the most widely used probability analyses of extreme values in hydrologic and meteorological studies for prediction of flood peaks and maximum rainfalls was used to estimate the temporal probability of occurrence of flood events in the area. Accordingly, the objective of frequency analysis was to find out discharges at different return periods using extreme value distribution by Gumbel method (Manandhar 2010, Van Westen et al. 2011) as mentioned below.

The annual maximum flood values were arraigned from low to high (ascending order) and assigned lowest rank 1 to the lowest value and assigned the highest rank N to the highest data value. Left sided probability of each event was calculated by equation 2 (Van Westen et al. 2011).

$$P_L = \frac{R}{N+1} \qquad \text{Equation (2)}$$

Where,

PL = Left side probability (probability of having less values in the series)
R = Rank
N = Total number of observations/ Numbers of years

The T (return period/ recurrence interval) was calculated for each observation by equation 3 (Van Westen et al. 2011).

$$T = \frac{1}{PR} = \frac{1}{1 - PL}$$ Equation (3)

Plotting position for each observation was calculated by equation 4 (Van Westen et al., 2011).

$$Y = -\ln(-\ln P_L)$$ Equation (4)

## Methodology

### *Study Area*

The Kelani River is the second largest river and the third largest watershed in Sri Lanka. It is also the fourth-longest river in Sri Lanka (Mallawatantri et al. 2016). This river basin is located totally in the wet zone of the country. The Kelani river basin receives an average annual rainfall of 3,450 mm and corresponding to a volume of about 7860 MCM out of which nearly 43 per cent discharges into the sea (Ministry of Irrigation & Water Resource Management 2018). The Kelani river basin is located at the coordinates between Northern latitudes 6° 46′ & 7° 05′ and Eastern longitudes 79° 52′ & 80° 13′ (De Silva et al. 2016). With the experience of the previous flood records of the Kelani river basin, the downstream or lower reach of the Kelani river basin was selected as the study area of this study. The absolute and relative location of the study area is illustrated in Figure 3.

**Figure 3.** *Absolute and Relative Location of the Study Area*

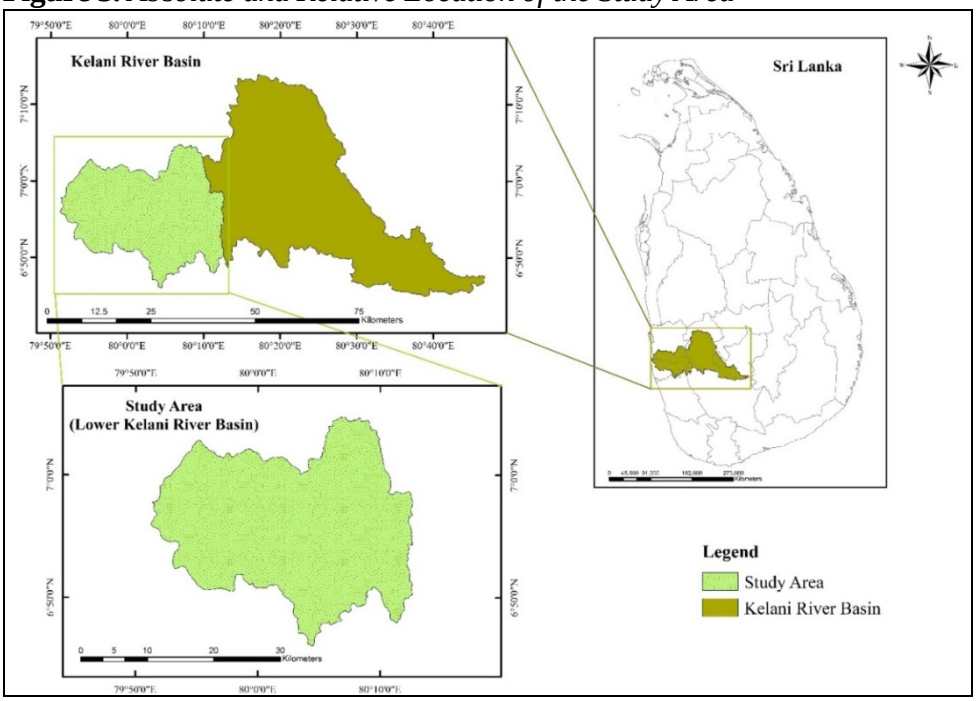


According to Figure 3, the selected study area is in the Western and Sabaragamuwa provinces of Sri Lanka and located at the coordinates between

Northern latitudes 6° 46′ & 7° 05′ and Eastern longitudes 79° 52′ & 80° 13′. Accordingly, the study area covers the flood plains below Glencourse gauging station in Kegalle district up to the Nagalagam Street gauging station in Colombo district. The total length of the Kelani river in the study area is about 55 kilometers. The total land area of the study area is about 810 square kilometers. The study area is in the wet zone of Sri Lanka and, it receives an annual rainfall varying from 500 mm to 4,000 mm with an average mean annual rainfall of about 2,440 mm over the elevation range of the basin.

### *Data Used for the Study*

The study was mainly based on secondary data. As hydrological data, daily discharge data were gathered for a period of 30-years between 1990 and 2019 from the Department of Irrigation, Sri Lanka to estimate the temporal probability of occurrence of flood events in the study area. Similarly, these hydrological data were collected from the Hanwella gauging station, which is located downstream of the Kelani river basin.

Different reports, press statements, annual reports, annual symposium proceedings, and other documents both published and unpublished by the relevant authorities including Disaster Management Centre, Ministry of Agriculture, as well as other local and international organizations, were used to identify the flood profile of the country containing the study area and its impacts. Further, other related literature such as books, journals, technical reports, and research papers were referred from different sources such as libraries and the World Wide Web through the Internet. Information found in the newspapers was also used.

### *Data Analysis Methods*

To estimate the temporal probability of occurrence of flood events, stream flow analysis by using normal distribution, trend analysis by using regression method and flood frequency analysis by using Gumbel's extreme value distribution were used.

## Results and Discussion

### *Stream Flow Analysis*

The normal distribution analysis and trend analysis were conducted to identify the stream flow pattern in downstream of the Kelani river basin. The mean of daily and monthly discharge data of each year was used as the descriptive statistic to determine the normal distribution of stream flow in the study area. Trend analysis was conducted using monthly average discharge data based on the regression analysis method (Sharma et al. 2018). Therefore, the monthly average discharges for the period from 1990 to 2019 are represented in Figure 4. According to Figure 4, there was two peaks in the year, which reveals the bi-

modal pattern of discharge in downstream of the Kelani river basin occurred in June (175 $m^3/s$) and in October (205 $m^3/s$). The annual average discharge of the river basin was 113 $m^3/s$.

**Figure 4.** *Monthly Average Discharge (1990–2019)*

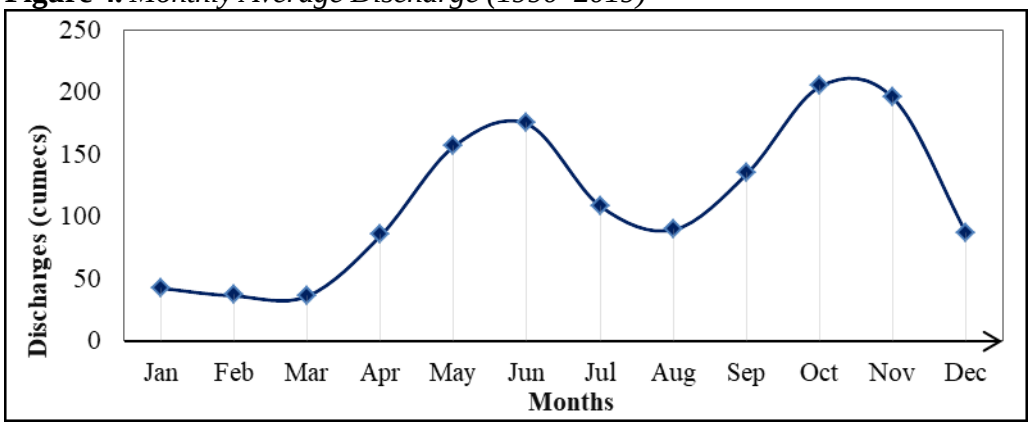


The result of time series trend analysis was indicated that a decreasing (negative) trend in monthly average discharges over the period (Figure 5). During the period, the maximum average discharge was recorded in 2016 with the average discharge of 528.66 $m^3/s$ in May while the lowest was recorded in the year 1992 with the average discharge of 15.26 $m^3/s$ in March.

**Figure 5.** *Monthly Average Discharges of Kelani River at Hanwella*

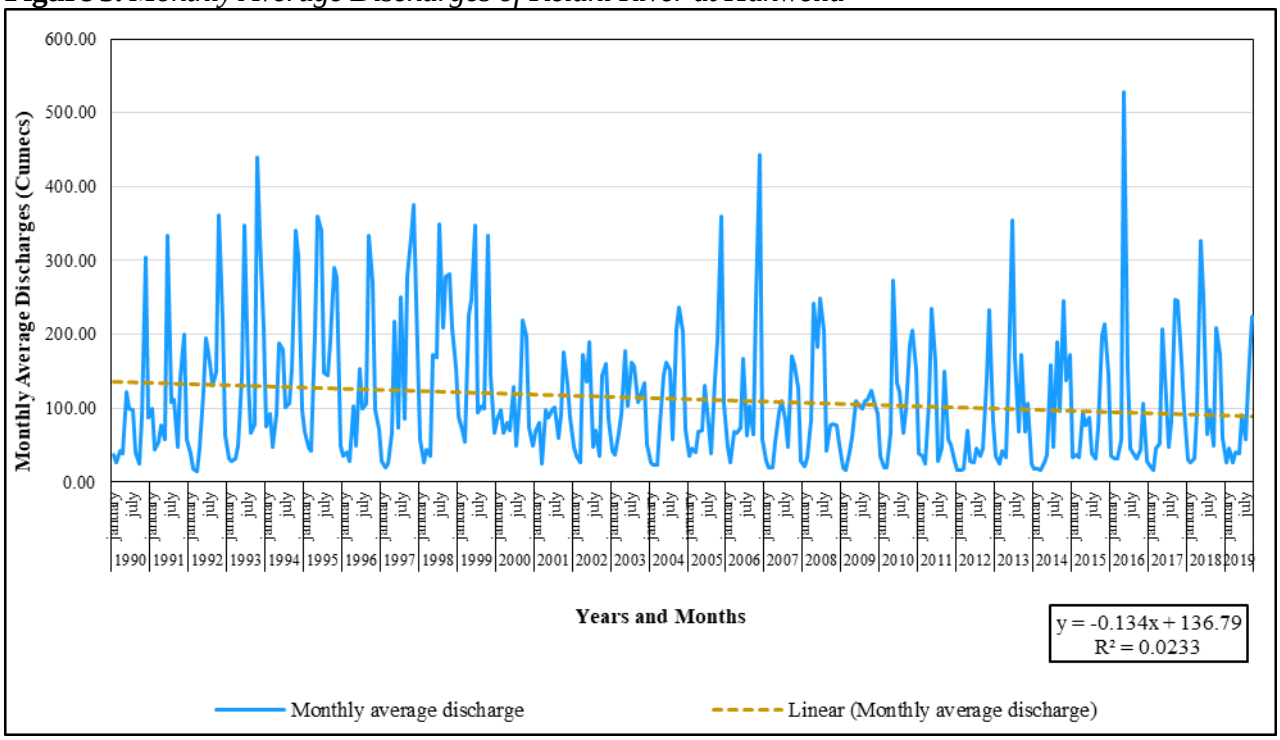

According to Figure 5, it is also evidenced that there were many variables in discharges of the Kelani river over the study area during the period between 1990 and 2019. The significant increases of discharges in the graph were indicated the flood hazard events in the study area. Therefore, it is important to calculate the probability of occurrence of historical flood magnitudes and return periods to assess flood risk (Yadav 2002, Sharma et al. 2018).

*Flood Frequency Analysis*

The objective of flood frequency analysis was to calculate the magnitude of extreme events at their frequency of occurrence using probability distributions (Yadav 2002, Sharma et al. 2018). Accordingly, the results of the flood frequency analysis are shown in Figure 6 and Table 3. Figure 6 shows the plotting positions of the discharges while Table 3 shows the calculation steps of flood frequency based on Gumbel's distribution method (Manandhar 2010).

**Figure 6.** *Gumble Probability*

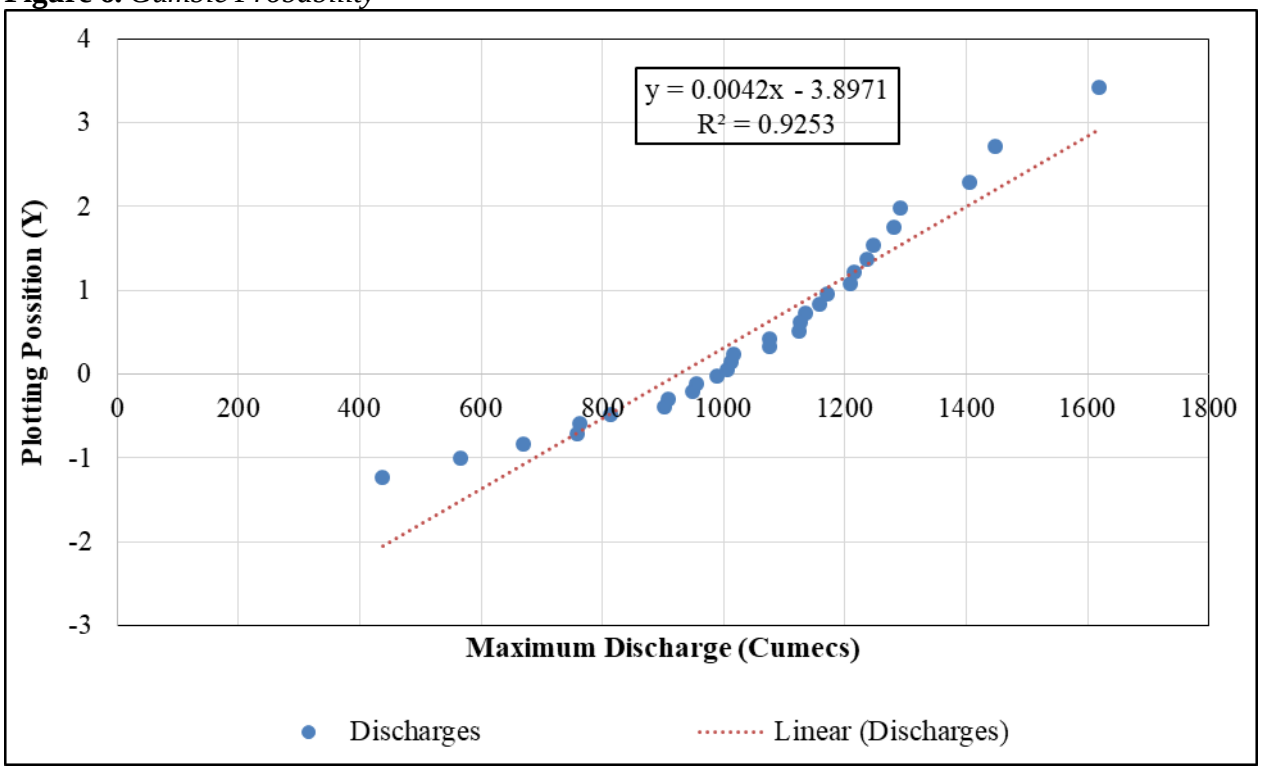


Accordingly, ten return periods were covered the total period of 30 years between the first and the last occurrence of high flood events as 1, 2, 3, 4, 5, 6, 8, 10, 16, and 31. The return periods and the probability of occurrence for each observation of downstream of the Kelani river basin are shown in Table 4.

Accordingly, as shown in Table 4, the study area had been affected ten times by low annual maximum discharges range between 439 $m^3/s$ and 956 $m^3/s$; eight times by discharges range between 957 $m^3/s$ and 1127 $m^3/s$; four times by discharges range between 1128 $m^3/s$ and 1210 $m^3/s$; two times by discharges range

between 1211 $m^3/s$ and 1238 $m^3/s$ with return periods of 1, 2, 3 and 4 years respectively. Therefore, the study area was experienced with a very high and high probability of flood occurrences with one and two-year-return periods. In other words, it was observed that there was a 97 per cent probability of flood occurrence almost annually and a 64 per cent probability of occurring once every two years. The study area was also experienced with a moderate probability of occurrences of three and four years return period floods. Further, the results were revealed that there was a less probability of occurrence of 5, 6, 8, 10, 16, and 31 years return period floods with relatively high discharge data.

**Table 4.** *Maximum Peak Discharges for Various Return Periods at Hanwella*

| Annual maximum discharges (Cumecs/ $m^3/s$) | Frequency | Return period | Probability of occurrence | Hazard level |
|---|---|---|---|---|
| 439 - 956 | 10 | 1 | 0.968 | Very High |
| 957 - 1127 | 8 | 2 | 0.645 | High |
| 1128 - 1210 | 4 | 3 | 0.387 | Moderate |
| 1211 - 1238 | 2 | 4 | 0.258 | Moderate |
| 1239 - 1247 | 1 | 5 | 0.194 | Low |
| 1248 - 1282 | 1 | 6 | 0.161 | Low |
| 1283 - 1292 | 1 | 8 | 0.129 | Low |
| 1293 - 1408 | 1 | 10 | 0.097 | Low |
| 1409 - 1449 | 1 | 16 | 0.065 | Very Low |
| > 1450 | 1 | 31 | 0.032 | Very Low |

Especially, the study area experienced several more severe flood events in the most recent, for example, the probability of occurrence of the 2016 flood at the same magnitude could be once in 31 years (probability = 0.032). Also, the return period of floods in 2017 was 15.5 years (Table 3). Accordingly, the results of flood frequency analysis of the study area can be used to design bridges, culverts, dams, and flood control structures for mitigating flood risk; to define flood plains; to determine the economic value of flood control projects and the effect of encroachments on the flood plain (Yadav 2002, Sharma et al. 2018).

**Table 3.** *Summary Table: Extreme Value Distribution by Gumbel Method*

| Year | Maximum Discharges in Cumecs | Re-arranged discharges | Rank (*R*) | $P_L$ | $P_R$ | Return Period (*T*) | Y |
|---|---|---|---|---|---|---|---|
| 1990 | 568 | 439 | 1 | 0.032258065 | 0.967741935 | 1.03 | -1.23372204 |
| 1991 | 1007 | 568 | 2 | 0.064516129 | 0.935483871 | 1.07 | -1.00826445 |
| 1992 | 1076 | 670 | 3 | 0.096774194 | 0.903225806 | 1.11 | -0.84817244 |
| 1993 | 1292 | 760 | 4 | 0.129032258 | 0.870967742 | 1.15 | -0.71671372 |
| 1994 | 1172 | 764 | 5 | 0.161290323 | 0.838709677 | 1.19 | -0.60133299 |
| 1995 | 764 | 814 | 6 | 0.193548387 | 0.806451613 | 1.24 | -0.4960537 |
| 1996 | 1135 | 904 | 7 | 0.225806452 | 0.774193548 | 1.29 | -0.39748472 |
| 1997 | 1216 | 910 | 8 | 0.258064516 | 0.741935484 | 1.35 | -0.30346609 |
| 1998 | 1017 | 950 | 9 | 0.290322581 | 0.709677419 | 1.41 | -0.21249718 |
| 1999 | 1282 | 956 | 10 | 0.322580645 | 0.677419355 | 1.48 | -0.12345767 |
| 2000 | 990 | 990 | 11 | 0.35483871 | 0.64516129 | 1.55 | -0.03545588 |
| 2001 | 670 | 1007 | 12 | 0.387096774 | 0.612903226 | 1.63 | 0.0522616 |
| 2002 | 760 | 1013 | 13 | 0.419354839 | 0.580645161 | 1.72 | 0.140368602 |
| 2003 | 814 | 1017 | 14 | 0.451612903 | 0.548387097 | 1.82 | 0.229501376 |
| 2004 | 904 | 1076 | 15 | 0.483870968 | 0.516129032 | 1.94 | 0.32029204 |

| | | | | | | | |
|---|---|---|---|---|---|---|---|
| 2005 | 950 | 1076 | 16 | 0.516129032 | 0.483870968 | 2.07 | 0.413398773 |
| 2006 | 1210 | 1125 | 17 | 0.548387097 | 0.451612903 | 2.21 | 0.509536687 |
| 2007 | 1076 | 1127 | 18 | 0.580645161 | 0.419354839 | 2.38 | 0.609513182 |
| 2008 | 1408 | 1135 | 19 | 0.612903226 | 0.387096774 | 2.58 | 0.714272302 |
| 2009 | 910 | 1159 | 20 | 0.64516129 | 0.35483871 | 2.82 | 0.824954504 |
| 2010 | 956 | 1172 | 21 | 0.677419355 | 0.322580645 | 3.10 | 0.942981875 |
| 2011 | 1247 | 1210 | 22 | 0.709677419 | 0.290322581 | 3.44 | 1.07018592 |
| 2012 | 439 | 1216 | 23 | 0.741935484 | 0.258064516 | 3.88 | 1.209008835 |
| 2013 | 1159 | 1238 | 24 | 0.774193548 | 0.225806452 | 4.43 | 1.362838126 |
| 2014 | 1125 | 1247 | 25 | 0.806451613 | 0.193548387 | 5.17 | 1.53659934 |
| 2015 | 1013 | 1282 | 26 | 0.838709677 | 0.161290323 | 6.20 | 1.73789269 |
| 2016 | 1620 | 1292 | 27 | 0.870967742 | 0.129032258 | 7.75 | 1.979412778 |
| 2017 | 1449 | 1408 | 28 | 0.903225806 | 0.096774194 | 10.33 | 2.284915186 |
| 2018 | 1238 | 1449 | 29 | 0.935483871 | 0.064516129 | 15.50 | 2.707679652 |
| 2019 | 1127 | 1620 | 30 | 0.967741935 | 0.032258065 | 31.00 | 3.417637092 |

## Conclusion

When considering the Kelani river basin, it is recorded as a highest flood frequency and the accompanying flood damages among the river basins in wet zone. Specially, flood frequency is the concept of the probable frequency of occurrence of a given flood. For the design of engineering works, it is not sufficient to identify only the maximum observed flood, it is also necessary to find out the frequency of occurrence of the flood. Therefore, the specific objective of the study is to estimate the temporal probability of occurrence of flood events in downstream of Kelani river basin. The results of the study revealed that there was a bi-modal pattern of discharges that occurred in June and October. The results also indicated that ten return periods were covered the total period of 30 years between 1990 and 2019, and there was a 97 per cent probability of flood occurrence almost annually and 64 per cent probability of occurring once every two years.

According to the outcomes of the study, it can be said that stream flow and flood frequency analyses are important concepts and techniques for reducing flood damages in an area and for the designers of the flood control works. As well as flood frequency information can be applied to controlling land uses and settlements on flood prone areas and many other applications. This study, therefore, was recommended to design bridges, culverts, dams, and flood control structures for mitigating flood risk; to define flood plains and for modeling purposes; to determine the economic value of flood control projects and the effect of encroachments on the flood plains in downstream of the Kelani river basin.

## References

Baishya SJ (2013) Vulnerability assessment and management of flood hazard in Baralia River (Bhairatolajan): a case study of Khopanikuchi Village of Hajo Revenue Circle, Kamrup District Assam, http://www.ijirset.com.

Balabanova S, Vassilev V (2010) *Creation of flood hazard maps*. Paper presented at *4th BALWOIS Conference on Water Observation and Information System for Decision Support*. Available at: http://balwois.com/balwois/administration/full_paper/ffp-1560.pdf.

Basnayake S, Punyawardena BVR, Jayasinghe S, Gupta N, Shrestha ML, Premalal KHMS (2019) *Climate smart disaster risk reduction interventions in agriculture sector – Flood hazard – A report*. Available at: http://www.adpc.net/igo/category/ID1578/doc/2020-cHxj0N-ADPC-Report_Climate_Smart_DRR.pdf.

Consortium of Humanitarian Agencies (2016) *Impacts of disasters in Sri Lanka*. Sri Lanka: The Consortium of Humanitarian Agencies.

De Silva MMGTD, Weerakoon SB, Herath S (2016) Event-based flood inundation mapping under the impact of climate change: a case study in Lower Kelani River Basin, Sri Lanka. *Hydrology 7*(228): 1–24.

Department of Irrigation in Sri Lanka (2020) *Hydrological Annual of Sri Lanka 2019/ 2020.* Colombo 07: Sri Lanka.

Disaster Management Centre (1999) *Sri Lanka country report*. Available at: https://issuu.com/suzanne_brady/docs/sri_lanka_country_report.

Disaster Management Centre (2012) *Hazard Profiles of Sri Lanka.* Retrieved from http://www.dmc.gov.lk/hazard/hazard/Report.html.

Dissanayake P, Hettiarachichi S, Siriwardana C (2018) Increase in disaster risk due to inefficient environmental management, land use policies and relocation policies. Case studies from Sri Lanka. *Procedia Engineering* 212: 1326–1333.

European Community (2020) *Project flood site*. Oxford shire: Samui Design & Management Ltd.

Genovese E (2006) A methodological approach to land use-based flood damage assessment in urban areas: Prague case study. Italy: European Communities.

Gilard O (1996) Flood risk management: risk cartography for objective negotiations. In *3rd IHP/IAHS George Kovacs Colloquium*. UNESCO: Paris.

Hettiarachchi S (2020) Hydrological report on the Kelani River flood in May 2016. Available at: https://www.researchgate.net/publication/342865359_Hydrological_Report_on_the_Kelani_River_Flood_in_May_2016.

Hewitt K (2013) Environmental disasters in social context: toward a preventive and precautionary approach. *Nat Hazards* 66: 3–14.

Jayawardena S, Darshika T, Herath R (2017) Observed climate trends, future climate change projections and possible impacts for Sri Lanka. *NeelaHaritha – The Climate Change Magazine of Sri Lanka* 2: 144–151.

Jegarasasingam V (2017) *Sri Lanka country report*. Available at: http://www.adrc.asia/countryreport/LKA/LKAeng98/.

Klijn F (Ed.) (2009) *Flood risk assessment and flood risk management: an introduction and guidance based on experience and findings of FLOOD site (an EU-funded Integrated Project)*. Delft: Deltares, Delft Hydraulics.

Mallawatantri A, Goonatilake SDA, Perera N, Silva GD, Weerakoon D (2016) *Natural resource profile of the Kelani River basin*. Colombo: International Union for Conservation of Nature Sri Lanka Country Office and Central Environment Authority.

Manandhar B (2010) *Flood Plain Analysis and Risk Assessment of Lothar Khola*. Master of Science Thesis. Nepal: Tribhuvan University.

Ministry of Disaster Management (2016) *Sri Lanka post-disaster needs assessment: floods and landslides-May 2016*. Available at: https://reliefweb.int/sites/relief web.int/files/ resources/pda-2016-srilanka.pdf.

Ministry of Irrigation & Water Resource Management (2018) *Strategic environmental assessment of development of River Basin level flood and drought mitigation investment plans-Kelani River Basin*. Kotte: Sri Lanka.

Perera KKE (2017) The socio-economic impacts of flood disaster in Sri Lanka. *NeelaHaritha – The Climate Change Magazine of Sri Lanka* 2: 8–16.

Sharma KP, Adhikari NR, Ghimire PK, Chapagain PS (2018) GIS-based flood risk zoning of the Khando River basin in the Terai region of East Nepal. *Himalayan Journal of Sciences* 1(2): 103–106.

United Nations Development Programme (2011) *Practitioners' Guidebook on the best agricultural practices for drought and floods in Sri Lanka*. UNDP: Sri Lanka.

United Nations International Strategy for Disaster Reduction (2017) *The human cost of weather-related disasters 1995-2015*. Geneva: Switzerland.

United Nations Office for Disaster Risk Reduction (2019) *Disaster risk reduction in Sri Lanka: status report 2019*. Bangkok, Thailand.

United States Geological Survey (2020) *Floods: Recurrence intervals and 100-year floods*. Virginia: USA. Available at: http://ga.water.usgs.gov/edu/100yearflood.Flo ods.html.

UN-Water (2006) *Sri Lanka national water development report*. UNESCO.

Urban Development Authority (2019) *Homagama development plan (2019 – 2030)*, Battaramulla: Sri Lanka.

Van Westen CJ, Alkema D, Damen MCJ, Kerle N, Kingma NC (2011) *Multi-hazard risk assessment distance education course guidebook*. Twente: United Nations University-ITC School on Disaster Geoinformation Management (UNU-ITC DGIM).

World Meteorological Organization (2008) *Integrated flood management tools series No.20: flood mapping*. Geneva, Switzerland: World Meteorological Organization.

Yadav SK (2002) *Hydrological analysis for Bheri-babai hydropower project Nepal*. Master of Science Thesis. Norway: Norwegian University of Science and Technology, Department of Hydraulic and Environmental Engineering.

Yoshitani J, Takemoto N, Merabtene T (2007) *Factor analysis of water-related disasters in Sri Lanka*. Japan: The International Centre for Water Hazard and Risk Management.

Zubair L, Ralapanawe V, Yahiya Z, Perera R, Tennakoon U, Chandimala J (2020) *Fine scale natural hazard risk and vulnerability identification informed by climate*. Available at: https://www.semanticscholar.org/paper/Fine-Scale-Natural-Hazard-Risk-and-Vulnerability-by-Zubair Ralapanawe/5ad41350ebeec130f406bc95c9be5 29720e66035?p2df.